

# Design and Evaluation of Candidate Pressure Ports for the HYFLITE Experiment

John E. Teter, Jr., and Craig S. Cleckner  
*Langley Research Center, Hampton, Virginia*

Alfred E. Von Theumer  
*Lockheed Engineering & Sciences Company, Hampton, Virginia*

(NASA-TM-109146) DESIGN AND  
EVALUATION OF CANDIDATE PRESSURE  
PORTS FOR THE HYFLITE EXPERIMENT  
(NASA. Langley Research Center)  
69 p

N95-1

Unclassified

3/19 00203

July 1994

National Aeronautics and  
Space Administration  
Langley Research Center  
Hampton, Virginia 23681-0001



## Table of Contents

<b>SUMMARY .....</b>	<b>1</b>
<b>INTRODUCTION .....</b>	<b>2</b>
<b>OBJECTIVES .....</b>	<b>3</b>
<b>DESIGN DEVELOPMENT .....</b>	<b>4</b>
Requirements .....	4
Concept Development .....	4
Design Concept .....	5
Material Selection .....	6
Thermal Analysis .....	7
<b>PRESSURE PORT FABRICATION AND ASSEMBLY .....</b>	<b>9</b>
Tile Coring .....	9
Quartz Tube Fabrication .....	9
Fixed Pressure Port Assembly .....	10
Adjustable Pressure Port Assembly .....	11
<b>VIBRO-ACOUSTIC DESIGN VERIFICATION .....</b>	<b>12</b>
<b>AERO-THERMAL DESIGN VERIFICATION .....</b>	<b>12</b>
Aero-Thermal Test Facility .....	12
Aero-Thermal Test Results .....	13
Aero-Thermal Post-Test Tile Analysis .....	15
<b>CONCLUSIONS .....</b>	<b>16</b>
Vibro-Acoustic .....	16
Aero-Thermal .....	16
<b>FUTURE DEVELOPMENT .....</b>	<b>17</b>
Aero-Thermal Tests .....	17
Structural Testing .....	18
Method of Placement in Tile .....	18
Simplify Design .....	18
Strain Isolation Pad .....	18

## Tables

Table I. Material Selection.....	20
Table II. Summary of Test Sites.....	20
Table III. Data summary of test specimen thermocouples at 90 and 305 seconds.....	21

## Figures

Figure 1. Pressure Port initial concept.....	23
Figure 2. Pressure Port using only heat shrink tubing .....	24
Figure 3. Final design of the Fixed Pressure Port.....	25
Figure 4. Final design of the Adjustable Pressure Port.....	26
Figure 5. HYFLITE Pressure Port thermal model .....	27
Figure 6. HYFLITE BLT14H - Isentropic ramp heating .....	28
Figure 7. HYFLITE BLT14H - Variation of quartz tube temperature with depth .....	29
Figure 8. HYFLITE BLT14H - Variation of tile temperature with depth.....	30
Figure 9. HYFLITE BLT14H - Variation of holder temperature with depth.....	31
Figure 10. Tile core detail.....	32
Figure 11. Drawing of the quartz tube .....	33
Figure 12. Random vibration test spectrum for HYFLITE specimen .....	34
Figure 13. Vibration test input spectrum.....	35
Figure 14. Desired aero-thermal test temperature profile.....	36
Figure 15. Ames 2x9 Turbulent Flow Duct Facility .....	37
Figure 16. Aerial view of Thermophysics Test Facility .....	38
Figure 17. Isometric view of the test specimen .....	39
Figure 18. Schematic bottom view of the test specimen .....	40
Figure 19. Schematic cross section of test specimen.....	41
Figure 20. HYFLITE test article layout .....	42
Figure 21. Side view of test assembly prior to aero-thermal test .....	43
Figure 22. Top view of test assembly prior to aero-thermal test .....	44
Figure 23. Typical Model Installation in 2x9 Turbulent Flow Duct.....	45
Figure 24. Test assembly during calibration run .....	46
Figure 25. Tile thermocouple locations .....	47
Figure 26. Plot of pyrometer data, pyrometer located on the opposite wall of the test chamber.....	48
Figure 27. Plot of average chamber pressure, sensors located on the opposite wall of the test chamber .....	49
Figure 28. Plot of chamber heat flux, calorimeters located on the opposite wall of the test chamber .....	50
Figure 29. Plot of surface thermocouples, thermocouples located upwind of test specimen .....	51
Figure 30. Plot of tile thermocouple temperatures, thermocouples located .1" from tile surface except T/C 10 located .5" from tile surface .....	52
Figure 31. Plot of pressure port thermocouple temperatures .....	53

Figure 32. Plot of site #4 calorimeter plate thermocouple temperatures.....	54
Figure 33. Isometric view of post-test tile.....	55
Figure 34. Close-up of site #1 after aero-thermal test.....	56
Figure 35. Close-up of site #2 after aero-thermal test.....	56
Figure 36. Close-up of site #3 after aero-thermal test.....	56
Figure 37. Close-up of site #4 after aero-thermal test.....	56
Figure 38. Calorimeter plate.....	57
Figure 39. Cross section of the tile through site #2.....	58
Figure 40. Cross section of the tile through site #3.....	59
Figure 41. Close-up cross section of site #3.....	60
Figure 42. Close-up cross section of site #2.....	61
Figure 43. Close-up cross section of thermocouple 9.....	62
Figure 44. Close-up cross section of site #4.....	63

## Acronyms

ARC	Ames Research Center
AfE	Aeroassist Flight Experiment
BLT	Boundary Layer Transition
FRCI	Fibrous Refractory Composite Insulation
FTE	Flight Test Experiment
HYFLITE	HYpersonic FLIghT Experiment
LaRC	Langley Research Center
NASA	National Aeronautics and Space Administration
NASP	National AeroSpace Plane
RSI	Reusable Surface Insulation
RTV	Room Temperature Vulcanization
SINDA	Systems Improved Numerical Differencing Analyzer
SIP	Strain Isolation Pad
TEOS	Tetra-Ethyl-Ortho-Silicate
TMM	Thermal Math Model
TPS	Thermal Protection System
TUFI	Toughened Uni-piece Fibrous Insulation

## SUMMARY

The pressure port development consisted of a series of analyses and tests of candidate pressure sensing concepts that were capable of providing accurate pressure data acquisition for the HYpersonic FLIghT Experiment (HYFLITE). Significant activities, findings, and discussions are found in the subsequent sections of this report. Initial vibro-acoustic and aero-thermal testing of the pressure port designs have been completed at Langley Research Center (LaRC) vibration laboratory and the 20 MWatt 2 x 2 turbulent duct facility at Ames Research Center (ARC). The designs utilized two different configurations and two different bonding techniques which were evaluated for compatibility with FRCI-12 insulation tiles at 2800 degrees F surface temperature. The vibro-acoustical and aero-thermal performances of the pressure ports were found to be well within the required design limits for all cases.

Two failure mode tests were also performed at the above temperature to evaluate the effects of a protruding pressure port above the tile surface and a simulated failed bond where the whole instrument assembly was removed. Both failure modes proved to be benign relative to the Thermal Protection System (TPS) performance and sub structure heating. The protruding quartz tube tip melted and deformed slightly due to impinging hot gases. No other damage to the instrumentation was observed. A few post-test fractures on the tile and its coating were noticed which are most likely due to thermal stress. While no further damage to the interior of the Reusable Surface Insulation (RSI) was observed, this problem should be alleviated by using a Strain Isolation Pad (SIP) between the tile and the supporting structure.

## INTRODUCTION

The HYFLITE program is designed to provide early access to the hypersonic flow regime in preparation for the development of a National AeroSpace Plane(NASP) vehicle. The HYFLITE program consists of two separate flight experiments.

The first experiment is called the Boundary Layer Transition (BLT) experiment. It consists of a wedge-shaped vehicle that will be propelled to hypersonic speeds using a rocket. One side of the wedge will be a constant-slope ramp, while the other side will approximate an isentropic ramp. Both sides will be heavily instrumented with pressure sensors, acoustic microphones, thin film gages and thermocouples. The data acquired will provide information about the boundary layer transition from laminar to turbulent flow which will be used to correlate the baseline NASP computational tools, methodologies, and criteria. This experiment will also provide an opportunity to flight test instrumentation that is being developed for use on the NASP vehicle.

The second experiment is called the SCRAMJET Flight Test Experiment (FTE). In this experiment a scaled scramjet engine of NASP-like design will be lofted aboard a rocket to hypersonic speeds where it will be fueled and ignited. This experiment will provide flight test data to determine scramjet operation and performance at high hypersonic speeds. The data will also be used to determine engine inlet operation and performance. As with the first experiment, this vehicle will also be heavily instrumented with pressure transducers, acoustic microphones, thin film gages and thermocouples.

This report describes the design evolution and verification testing of the pressure transducers intended for the HYFLITE experiments. It specifically covers the design details, thermal analyses, vibro-acoustic testing and arc-jet testing of two candidate pressure transducer designs. Also included are details of the assembly process and observations regarding the assembly and testing of the designs.



## OBJECTIVES

The objective of the pressure transducer development effort was to install a pressure transducer with frequency response greater than 10 hertz into a piece of typical shuttle tile. The integration of the transducer also had to pose no risk to the Thermal Protection System (TPS) of the vehicle from either a structural or a thermal point of view. The assessment of risk to the TPS included any transducer failure modes which could possibly occur.

The test program was developed to evaluate the pressure transducer concepts included vibro-acoustic testing and arc-jet testing. The test article included samples of both candidate transducer designs as well as two failure mode samples.

The first failure mode included was really only applicable to the arc-jet testing. It was an open 0.100" diameter hole through the TPS tile which would simulate the complete loss of a pressure transducer. Such a hole could allow hot gases to be ingested into the vehicle. Although unlikely, this type of failure mode was included to evaluate the effects on the surrounding TPS and the internal structure of the vehicle.

The second failure mode was also only of concern in the arc-jet test. It was a quartz tube protruding above the surface of the tile. The protruding quartz tube was an unintentional failure mode caused inadvertently by an attempt to lengthen the threaded portion of the holder. After the holder was bonded into the TPS tile, it was discovered that the threads in the holder were not deep enough to accept the pressure transducer, so an attempt was made to tap more threads. The tap was threaded too deep into the blind hole and deformed the bottom of the holder causing the quartz tube to debond and protrude 0.026" above the surface of the tile (see Figure 42). A protruding quartz tube would experience much greater heating, and could cause local deformation.

## **DESIGN DEVELOPMENT**

### **Requirements**

Several mechanical and thermal requirements were imposed on the design:

Requirements to meet the 10 Hz dynamic response criteria:

- The tip of the pressure transducer cannot be more than .5" below the surface of the tile.
- Minimize discontinuities and the internal volume of the tube.
- Air tight seal between the pressure transducer and the holder.

Thermal requirements:

- The temperature of the tip of the transducer cannot exceed 250°F (121°C).
- The temperature should remain as uniform as possible along the length of the pressure transducer.
- Materials at the surface of the tile must withstand 2800°F (1538°C).

Requirements to meet .020" step and gap criteria:

- The maximum inside diameter of the tube is .020".
- The tube cannot protrude or recede more than .020" from the surface of the tile.

HYFLITE requirements:

- Minimize weight.
- Maintain the structural and thermal integrity of the TPS.
- No Strain Isolation Pad (SIP), (driven by .020" step/gap criteria).

### **Concept Development**

The design requirements for the HYFLITE TPS pressure port penetrations were quite similar to those of the Aeroassist Flight Experiment (AFE)<sup>1</sup>. As a result, the HYFLITE design developed from the AFE heritage. The major difference between the AFE design and the HYFLITE design was that the AFE pressure transducers were

remotely located, while the HYFLITE transducers had to be mounted within 0.50" of the tile surface due to frequency response considerations.

The original HYFLITE pressure port concept is shown in figure 1. A quartz tube was held in place by threading the pressure transducer until it seated the quartz tube against the holder. An O-ring between the quartz tube and the pressure transducer tip sealed the interface and allowed for thermal expansion of the holder.

This concept was abandoned for several reasons. First the tolerances and dimensions required were prohibitively small. There was a concern that the quartz tube may break or the tip of the pressure transducer may be damaged because of the metal to glass interface.

The next concept (see figure 2) was to hold the quartz tube on the end of the pressure transducer tip by a piece of heat shrink tubing. This simplified the design and allowed flexibility between the quartz tube and the transducer tip.

Thermal analysis showed that high rates of heat transfer along the quartz and into the transducer head would raise the transducer head beyond the acceptable temperature limits of an Endevco 8510 transducer. Parametric studies showed the best thermal characteristics were achieved if both the bottom and sides of the quartz tube contacted the metal holder and the quartz did not directly contact the transducer tip. An Endevco 8540 high temperature transducer was chosen after these analyses because of its broader temperature range. The Endevco 8540 also had a longer transducer tip which simplified the mechanical design because the transducer body did not have to be located in the tile but could be located slightly behind it.

## **Design Concept**

The final concept is shown in figure 3. A 0.5" long quartz tube is recessed .005" below the surface of the tile. The bottom of the quartz tube rests on a counter bore in the aluminum holder. RTV-560 on the sides and flange of the quartz tube holds the tube in

place and seals the connection. The compliance of the RTV-560 allows for thermal expansion of the holder. A .040" diameter chamfer (countersink) in the .020" diameter hole in the holder allows for small misalignments of the quartz tube in the counterbore. Either teflon or viton heat shrink tubing is shrunk around the body of the holder and the flange of the quartz tube. The tubing seals the connection and provides mechanical redundancy for the RTV-560 bond. Aluminum foil adhesive tape is wrapped around the outside of the shrink tubing as a thermal isolation against radiated heat from the tile. The holder is potted in place with RTV-560. Flats on the holder allow it to be held firmly in place with a wrench as the pressure transducer is inserted and torqued. This is necessary because the RTV-560 bond and the tile material are not strong enough to withstand the torque required. An O-ring on the top of the holder seats against a spacer. The thickness of the spacer is determined by measuring the length of the pressure transducer tip and the depth of the hole and allowing a .001" gap (see Figure 3). A second O-ring in the pressure transducer seats against the other side of the spacer.

Two concepts to position the transducer assembly in the tile were evaluated. One concept was to use RTV-560 as a shim between the holder flange and the tile counterbore (see figure 3). The advantage of this is simplicity. A disadvantage is the RTV-560 may creep with time and temperature. Another disadvantage is the difficulty of positioning the tip of the quartz tube because of irregularities in the tile surface.

Another concept (see Figure 4) was to allow the pressure transducer holder to screw in and out of the flange. The advantage of this concept is it does not depend on RTV-560 for positioning. The threaded holder offers a way to "dial in" the correct setting that the bond in place method does not. The disadvantage is increased complexity.

## **Material Selection**

Many different materials were used in this design. Most materials were space qualified. Table I, summarizes the materials and the reasons they were chosen.

## Thermal Analysis

Evaluation of the design concepts was based largely on the results of thermal analyses. The thermal analyses were performed using a finite difference based heat transfer code known as the Systems Improved Numerical Differencing Analyzer (SINDA-85). The thermal math model (TMM) was developed in Patran 2.5, a pre and post processor for a variety of analysis codes. The TMM included three dimensional geometric effects, temperature and pressure varying thermal conductivities and temperature varying thermal capacitances. A plot of the pie-shaped, axisymmetric TMM is shown in Figure 5. Material properties were taken from the established orbiter TPS database that was also used for AFE. The model included reradiation to an earth-temperature sink as a boundary condition. Heating rates provided by McDonnell Douglas and NASA Ames were applied to the surface of the TPS tile as driving functions. The heating rates used were derived for the Boundary Layer Transition (BLT) experiment and were labeled as case BLT14H. Peak heating rates in this case approached 41 Btu/ft<sup>2</sup>-sec. A plot of the incident heat flux for BLT14H is shown in Figure 6. Results from these models compared favorably with test data from the HYFLITE material selection arc jet tests, and a test data-correlated analytical model at NASA Ames with a proven history.

Design requirements for the transducer restricted the peak temperature to be less than 250 degrees F during data acquisition at around 160 seconds into the flight. Quantitative restrictions on temperature gradients were not available at the time of the analyses. Qualitative restrictions were to minimize both the absolute temperature of the transducer and the gradients to which it was subjected.

The initial design concepts placed the quartz tube in direct contact with the tip of the pressure transducer (the transducer head). Thermal analysis using the SINDA-85 code predicted that conduction heat transfer along the quartz tube and into the transducer head

would quickly lead to an over-temperature situation for the transducer. The analysis predicted temperatures of approximately 300 degrees F at 160 seconds into the flight.

Parametric studies were performed to evaluate design trade-offs. The final two designs; the fixed and adjustable holder had much in common from a thermal point of view. Subsequent design improvements were centered around the holder.

In both designs the holder provides a seat for the quartz tube that prevents contact between the transducer head and the quartz tube. (See Figures 3,4) This improvement minimizes any radiative or conductive heat transfer from the quartz tube to the transducer head. This improvement also eliminates any potential damage to the transducer head by impacts or shocks to the quartz tube in the direct contact design. The conductive path to the transducer head is further minimized by the fact that the holder only contacts the transducer in the threaded region near the inner mold line; away from the surface and the transducer head. Also of benefit was the relatively large thermal mass of the aluminum holder, which provided additional thermal stability to the transducer head and minimized temperature gradients. Another improvement added to the designs was the addition of pressure sensitive adhesive foil tape to the exterior of the holder. The foil tape covered the heat shrink tubing which attached the quartz to the holder. This tape provided a reflective surface which minimized any radiative heat transfer from the relatively "hot" tile to the "cool" holder assembly.

Incorporating these design modifications, the TMM predicted that the transducer head would rise from room temperature to 145 degrees F at 160 seconds into the flight, while the surrounding tile temperatures were approximately 700 degrees F. Figures 7 through 9 display the temperature profiles predicted by the TMM for the various components of the system. Figure 7 displays the variation of temperatures along the quartz tube from the surface exposed to the flow down to the base in contact with the holder.

Figure 8 displays the variation of the tile temperatures with distance from the exposed surface. Figure 9 displays the relatively isothermal nature of the holder; that is, the lack of gradients along its length. Due to a lack of physical information, the pressure transducer itself was not explicitly modeled. However, it is conservative to assume that the pressure transducer follows the temperature profile of the aluminum holder.

## **PRESSURE PORT FABRICATION AND ASSEMBLY**

The metal pressure port parts were fabricated using common machining practices. The TPS tile was cored in the LaRC glass laboratory using special techniques. The pressure ports are assembled using standard practices as described later in this section.

### **Tile Coring**

The Toughened Uni-piece Fibrous Insulation (TUFİ) coated, and Tetra-Ethyl-Ortho-Silicate (TEOS) densified tiles were machined as follows:

- 1) The uncoated side of the tile was clamped to the plate on the milling machine.
- 2) The .100" diameter hole was drilled through the whole tile with a special sized diamond tool.
- 3) The tile was removed and clamped with the TUFİ coated side down to a fixture that aligned the coring tool with the .100" diameter hole as the pilot hole.
- 4) The tile was then cored as shown in figure 10 with a diamond drill bit within .30" of the surface of the tile.
- 5) Six .060" diameter holes were then drilled to within .10" of the tile surface and one hole of same diameter but .50" deep for thermo-couples (see figure 26).
- 6) The tile became saturated with deionized water used for the machining and drilling processes (no contaminating fluids or adhesives were used). The deionized water was removed by vacuum baking in an oven at 250 degrees for twelve hours.

## **Quartz Tube Fabrication**

Quartz tubes were produced as shown in figure 11 and ground to dimensions indicated. The pressure port length from the tip to the flange was critical.

## **Fixed Pressure Port Assembly**

The fixed pressure port was assembled as follows:

- 1) The quartz tube flange was fastened to the tip of the aluminum holder with RTV-560 and allowed to cure.
- 2) Shrink tubing was placed around the body of the holder and flange of the quartz tube and heated for shrinkage.
- 3) Adhesive aluminum foil tape was wrapped around the outside of the heat shrink tubing.
- 4) A thin layer of RTV-560 was spread on the bottom of the tile counterbore and the holder assembly was placed in the hole so that the quartz tube was recessed .005" from the TUFFI coated surface of the tile. Additional RTV-560 was added to fill the counterbore and was allowed to cure.
- 5) The length of the pressure transducer head and the depth of the hole in the holder were measured. A spacer was machined to provide .001" gap between the tip of the pressure transducer (transducer head) and the holder hole.
- 6) An O-ring was placed on both sides of the machined spacer. One was provided by Endevco to seal the transducer to the machined spacer. The other was provided by NASA and seals the machined spacer to the holder. The pressure transducer was threaded in until resistance was met, and both O-rings were seated.
- 7) While retaining the holder with a wrench, the pressure transducer was torqued to 15 in-lb.



## **Adjustable Pressure Port Assembly**

The adjustable pressure port was assembled as follows:

- 1) The stainless steel holder was screwed on the aluminum holder.
- 2) The quartz tube flange was potted in place on the tip of the aluminum holder and allowed to cure.
- 3) Shrink tubing was placed around the body of the holder and flange of the quartz tube and heated for shrinkage.
- 4) Adhesive aluminum foil tape was wrapped around the outside of the heat shrink tubing.
- 5) The assembly was placed in the counterbore of the tile and potted in place with RTV-560.
- 6) The assembly was threaded until the quartz tube was recessed .005" from the TUF1 coated surface of the tile. The external threads on the holder were staked in place with cyanocrylate (glyptal was not available).
- 7) The length of the pressure transducer head and the depth of hole in the holder were measured. A spacer was machined to allow a .001" gap between the tip of the pressure transducer (transducer head) and the bottom of the hole.
- 8) An O-ring was placed on both sides of the machined spacer. One was part of the transducer. It sealed the transducer to the machined spacer. The other O-ring was part of the holder. It sealed the machined spacer to the holder. The pressure transducer was threaded in until resistance was met, and both O-rings were seated.
- 9) While retaining the holder with a wrench, the pressure transducer was torqued to 15 in-lb.

## **VIBRO-ACOUSTIC DESIGN VERIFICATION**

A test was conducted to demonstrate that the HYFLITE tile/transducer assembly would not be damaged when subjected to anticipated flight random vibration environment. This determination was made by visual inspection after testing in each axis.

The weak point in the design was considered to be the brittle quartz tube. The inspection method was to apply masking tape to the end of the tube and perform a pull test. A broken tube would have been removed with the tape.

A specimen similar to the Arc Jet sample was bonded to a 2" thick aluminum plate which was then attached to a Unholtz-Dickie T-1000 shaker. Control was provided by 2 accelerometers attached to the 2" plate. Response at the pressure transducer was not monitored because the transducer sites did not lend themselves to accelerometer installation. The assembly was vibrated to the levels shown in Figure 12 in each of the 3 axes. Figure 13 is a plot of the actual input spectrum with the upper and lower control limits of  $\pm 3$  db. Pre and post test inspections revealed that all 3 test sites were unaffected by exposure to the vibration.

## **AERO-THERMAL DESIGN VERIFICATION**

One test run was performed at the ARC 20 MWatt Thermophysic Test Facility to evaluate the two candidate pressure port assembly designs: a fixed pressure port assembly, and an adjustable pressure port assembly. The purpose of this test was to verify the thermal and mechanical acceptability of the concepts. The tile was subjected to 2800°F at 2.1 psi for 60 seconds. The desired temperature profile is shown in figure 14.

### **Aero-Thermal Test Facility**

This aero-thermal test program was performed in the 2 x 9 in. turbulent supersonic flow duct test facility of the ARC thermo-physics test facilities (see figure 15). The test article was assembled on a 8" by 10" test panel and mounted in the duct wall. The

turbulent duct is driven by a 20 MWatt Huels type arc heater. The turbulent duct has calorimeters, pressure transducers and a pyrometer installed into the duct wall opposite the test article.

An aerial view of the arc jet facilities is shown in figure 16. The power supply employed for the turbulent duct facility is rated at 20 MWatt for approximate 75 minutes. The power supply is controlled at the control panel by means of a bias control which sets the current available from the saturable reactors. There is no direct voltage control. Voltage is regulated by the amount and quality of air or other test gases injected into the arc heater column.

The primary cooling is accomplished by water located in a 160,000 gallon storage tank with 40 feet head pressure. The water from the tank is deionized to reduce conductivity. This deionized water is used for cooling the arc heaters, model supports, nozzles, etc.

The data acquisition system was used in the "Static" mode. In this configuration, a set of data samples are scanned and averaged, yielding a single data point which is then recorded. These points comprise the data taken through the course of a test run. The fastest rate of acquisition in this mode is between two and three data points every second. The acquisition system has a "Real Time" display feature which provides line plots and digital readouts for selected channels and will accommodate up to five channel selections at a time.<sup>2</sup>

## **Aero-Thermal Test Results**

A calibration test (run #17) was performed to establish facility operating parameters. Then a 90 second thermal test (run #18) was performed. Data was recorded for 305 seconds in order to show transient thermal effects during the test and while the tile was cooling.

Figure 17 shows a photograph of the instrumented tile. Figures 18 and 19 show schematics of the tile with the four test locations. The four sites in the tile are described below

and are summarized in Table II. Sites 1, 2, 3 contained pressure port assemblies. Site 1 contained a fixed pressure port fitted with a live Endevco 8510 pressure transducer which recorded data during the test. A second Endevco 8510 was placed behind the tile to record background electrical noise. Site 2 contained an adjustable pressure port fitted with a dummy transducer. Prior to testing the port was accidentally damaged causing the quartz tube to protrude .026" from the surface of the tile (.020" is the maximum allowable). Site 3 contained a fixed pressure port fitted with a dummy transducer. Site 4 contained only a bored hole in the tile to simulate the loss of a pressure port through mechanical failure.

The test tile was bonded directly to an aluminum plate with RTV-560. No SIP was used. A second piece of tile was mounted to the back of the aluminum plate as a spacer to shim the assembly to 2" total thickness (see figure 20). This assembly was mounted downstream of an LI2000 tile. The LI2000 tile contained four surface thermocouples (T/C1 through T/C4). Both tiles were mounted to a 3/16" aluminum mounting plate. A side and top view of the assembly is shown before installation into the test chamber in figures 21 and 22, respectively. This assembly was mounted in the test chamber as shown in a typical installation in figure 23. Three pressurized cans were used to wire instrumentation to outside connectors. The assembly was located outside of the test chamber during the calibration run to check background electrical noise as shown in figure 24.

A pyrometer was located opposite the test specimen. Pressure transducers and calorimeters were located on the opposite wall of the test chamber. In addition 13 thermocouples (T/C 6 through T/C 19) were placed in various locations in the test specimen as shown in figure 25. Plots of pressure transducer, calorimeter, thermocouple and other data are shown in figures 26 through 32. Table III summarizes the test specimen thermal data at test shut down (90 seconds) and the end of the data take (305 seconds).

## Aero-Thermal Post-Test Tile Analysis

Figure 33 is a photograph of the post-test assembly. The yellow-brown color on the ends of quartz tubes and surface of the tile are copper deposits from the arc jet electrodes. Pressure ports 1 and 3 (figures 34 and 36) are unchanged with respect to geometry and location, except for the copper deposits on the tube surface.

Pressure port 2 demonstrated a benign failure mode. The quartz tube protruded .026" into the flow field as shown in figure 35. The leading edge of the quartz tube softened causing some distortion to occur along the outer surface of the tube but the orifice remained open and circular. The trailing edge of the port was chipped prior to testing and remained unchanged.

Site 4 (figure 37) demonstrated the benign effects of a complete loss of a pressure port. A calorimeter plate (figure 38) was installed .375" from the base plate to allow heating rates and temperatures behind the open port to be measured. The slug calorimeter plate is a .030 thick rectangular aluminum plate with two thermocouples attached to monitor the temperature of the plate. The temperature of the slug calorimeter plate never exceeded 230 degrees F. By using the time history plots and knowing the surface area, weight and specific heat at constant pressure of the slug calorimeter plate, the maximum heat flux was determined to be .27 Btu/ft<sup>2</sup>-sec. The heat flux through the open port is only a fraction of 170 Btu/ft<sup>2</sup>-sec seen by the chamber calorimeters and demonstrates the loss of a pressure port is a benign failure.

After inspection, the tile was tested for flatness. The surface of the tile was flat within .012" using a 616 node grid. This indicates that the tile did not deform significantly during the test. The tile was then sectioned in two locations: through the middle at pressure port 2 and close to one end at pressure port 3. The cross sections are illustrated in figures 39 through 44. Various discolorations in the tile cross-section were observed. These discolorations are usually due to various temperatures. Unfortunately the coolant (deionized water) used in the dissecting process makes the interpretation of the color strata somewhat obscure. Dirty gray

marks can either be caused by the deionized water coolant or temperature variations in the TUF material.

It should be noted that the higher thermal conductivity of the quartz tube conducted more heat into the interior of the tile, as evidenced by the chalky white discoloration of the TPS material surrounding the quartz tube.

The data from thermocouples T/C 6 through T/C 12 are suspect. The relatively large amount of RTV-560 used to pot the thermocouples in place affected the temperature by providing a thermal discontinuity and a local area of higher thermal mass. Figure 44 shows the local heating caused by the RTV-560 as evidenced by the bright white area. All other thermocouple measurements were unaffected by the RTV-560.

Several hairline fractures on the tile were also observed after the test. The fractures most likely occurred because of thermal stresses due to high temperature differentials. This problem can probably be alleviated by using a Strain Isolation Pad (SIP) between the tile and the base plate. SIP is not the baseline design currently because the instability of the SIP may exceed the .020 step and gap criteria for surface roughness.

## **CONCLUSIONS**

Two designs of a surface pressure measurement system were developed and successfully tested for use with a TUF coated FRCI-12 insulation tile. Testing included extensive vibro-acoustic and aero-thermal performance tests.

### **Vibro-Acoustic**

The test objectives of this programs were met. The vibro-acoustic performance data were obtained and all design configurations survived the prescribed tests successfully. No damages, separation of parts, or dimensional deformities were observed in any of the components of the pressure port penetration test assemblies. Thus the pressure port penetration system design was concluded to be acceptable.

## **Aero-Thermal**

All test objectives were achieved. The thermal performance data were acquired for both the fixed and the adjustable pressure port designs, to determine the compatibility of these designs with the TUF-I coated FRCI-12 insulation tile. These pressure port systems were found to have acceptable thermal performance for the surface temperature of 2800 degrees F and 0.1 atmospheres of pressure for the tile density of 12 pounds per cubic foot.

Two failure modes were evaluated and proved to be benign. In one failure mode, a pressure port assembly was completely removed from the tile to simulate flow from the surface of the vehicle to its interior. The test proved the complete loss of a pressure port would not endanger the vehicle or TPS. In the second failure mode a quartz tube protruded .026" above the surface of the tile. This potential hot spot also proved to be harmless to the vehicle and TPS.

Although a few fractures on the tile occurred, no evidence of overheating in the interior of the RSI was observed in the dissected pieces. An application of SMC would most likely alleviate the fracturing of the tile. The overall aero-thermal test performances were entirely satisfactory and this test program proved that these two design approaches are thermally acceptable candidates for the HYFLITE program.

## **FUTURE DEVELOPMENT**

### **Aero-Thermal Tests**

No further aero-thermal tests are necessary unless there are changes in the design requirements such as vehicle velocity, angle of attack, longevity of the flight, lower altitudes, etc.

## **Structural Testing**

Additional tests should be conducted to determine the structural integrity of the designs to prove that no catastrophic damage will occur to the thermal protection system. The structural tests should include a pullout test, a side load test and a torsion test.

## **Method of Placement in Tile**

A new method of recessing the quartz tube assembly .005" below the tile surface needs to be developed. The method now used is to place the tile upside down on a flat surface and then insert the quartz tube in the cored tile until it bottoms out against the flat surface. The problem is that the tile is not flat and it rests on the high spots. The best one can do is get the tube flush with the surface. Usually the tube sticks out. This will be a greater problem with tiles that are intentionally curved.

## **Simplify Design**

Another look should be taken at simplifying the design. It would be advantageous to reduce the part count. If the pressure transducer probe length and the holder hole can be held to close tolerance, the spacer and one O-ring may be eliminated.

## **Strain Isolation Pad**

SIP should be used between the tiles and vehicle structure to prevent strain on the thermal protection system.



## References

1. Von Theumer, Alfred, "Design and Evaluation of Candidate Pressure Distribution and Air Data System Tile Penetration for the Aeroassist Flight Experiment", NASA Contractor Report 4312, September 1990.
2. A. Balter-Peterson, "Arc Jet Testing in NASA Ames Research Center Thermophysics Facilities", AIAA-92-5041.

**Table I. Material Selection**

<b>Item</b>	<b>Material</b>	<b>Specification</b>	<b>Reasons Chose</b>
Tile	Thermal tile	TUFI coated FRCI-12	baseline, chosen by Ames Research Center
Tube	Quartz	Fused Silica/ Corning 7940	high melting point, inert
Holder	Aluminum	Al 6061-T6	ease of machining, readily available
Screw Type Holder Flange	Stainless steel	PH 17-4	dissimilar metal to aluminum, prevents galling, corrosion resistant
Adhesive	RTV	560	readily available, high temperature, space qualified
O-ring	Viton	MIL-R-83248 CL 1 (Parker V884-75)	high temperature, space qualified
Shrink Tubing	Viton	MIL-I-23053/13	high temperature, space qualified
	Teflon	Inner lining - FEP Outer Shell - TFE	high temperature, sealing properties
Staking Compound	Glyptal		durable, space qualified
Adhesive Foil Tape	Aluminum		readily available, good thermal properties, thin, flexible

**Table II. Summary of Test Sites.**

<b>Site</b>	<b>Description</b>	<b>Transducer</b>	<b>Tube Extension (inches)</b>
<b>#1</b>	<b>Fixed Pressure Port</b>	<b>Endevco 8510</b>	<b>.004</b>
<b>#2</b>	<b>Adjustable Pressure Port</b>	<b>Dummy</b>	<b>.006</b>
<b>#3</b>	<b>Fixed Pressure Port</b>	<b>Dummy</b>	<b>.024</b>
<b>#4</b>	<b>Failure Port</b>	<b>None</b>	<b>None</b>

**Table III. Data summary of test specimen thermocouples at 90 and 305 seconds**

<b>Designation</b>	<b>Location</b>	<b>Site #</b>	<b>Type *</b>	<b>90 sec deg F</b>	<b>305 sec deg F</b>
T/C 6	In tile - .1" from surface	1	R	-	-
T/C 7	In tile - .1" from surface	1	R	1611	364
T/C 8	In tile - .1" from surface	1	R	1630	593
T/C 9	In tile - .1" from surface	2	R	1815	558
T/C 10	In tile - .5" from surface	2	R	159	502
T/C 11	In tile - .1" from surface	2	R	2076	633
T/C 12	In tile - .1" from surface	3	R	1762	607
T/C 13	Static pressure port flange	1	K	104	218
T/C 14	Static pressure port dummy transducer	3	K	139	241
T/C 15	Failure port - calibration plate, center	4	K	171	216
T/C 16	Failure port - calibration plate, 1/4" from center	4	K	171	219
T/C 17	Static pressure port flange	3	K	100	213
T/C 18	Adjustable pressure port flange	2	K	91	213
T/C 19	Adjustable pressure port dummy transducer	2	K	95	220

\* Type R = Platinum - Platinum/13% Rhodium

Type K = Chromel - Alumel

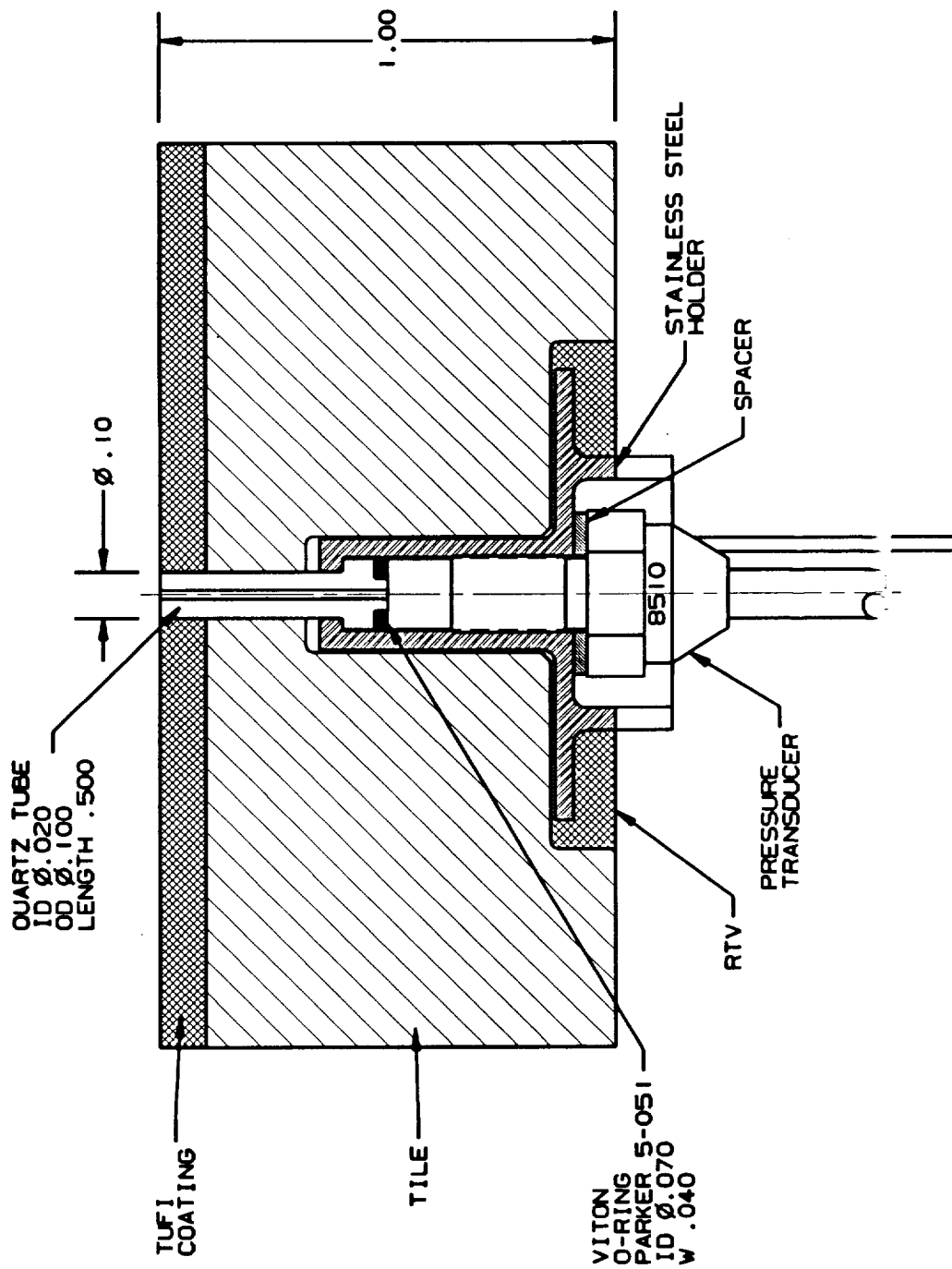


Figure 1. Pressure Port initial concept.

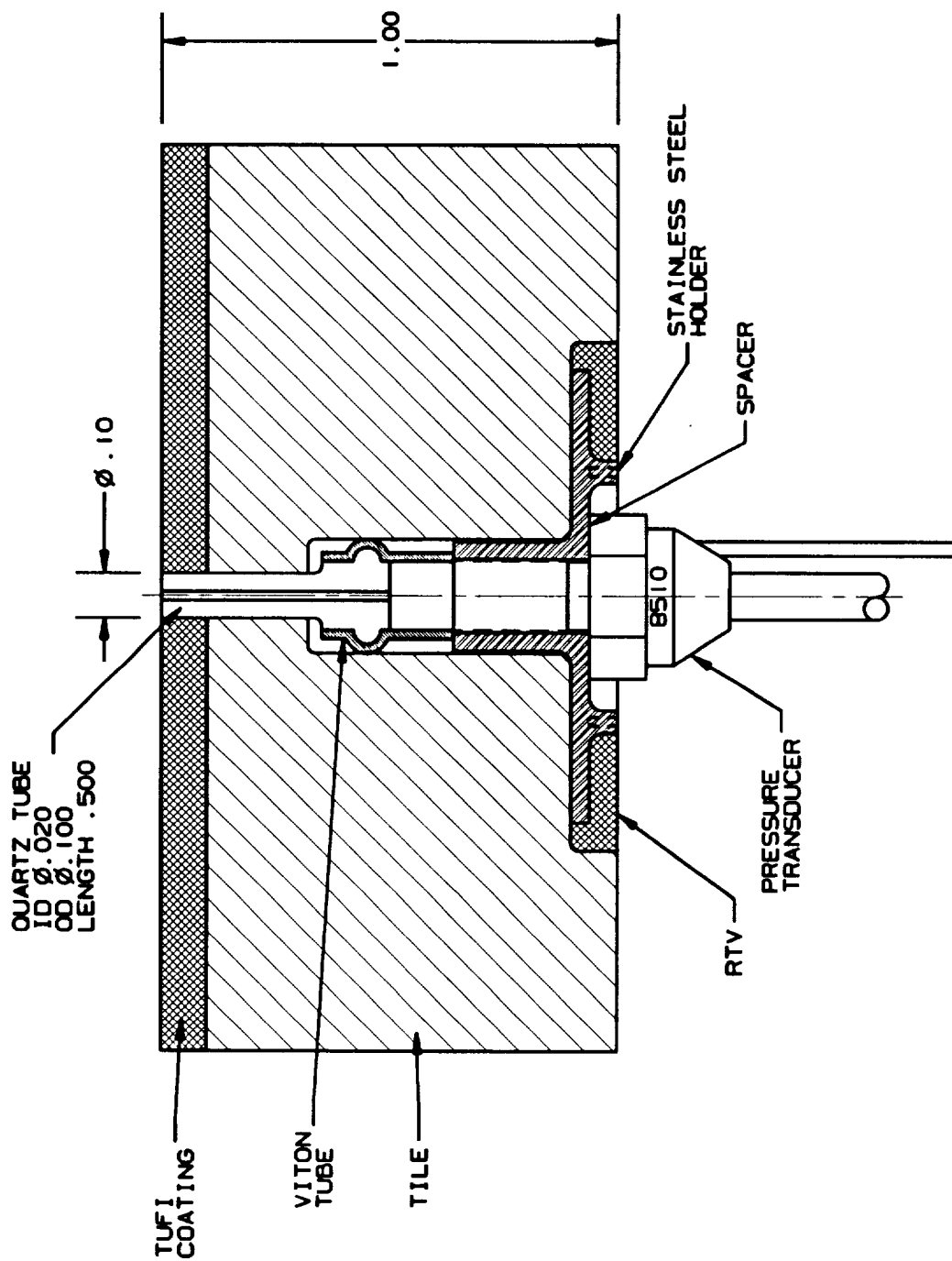


Figure 2. Pressure Port using only heat shrink tubing.

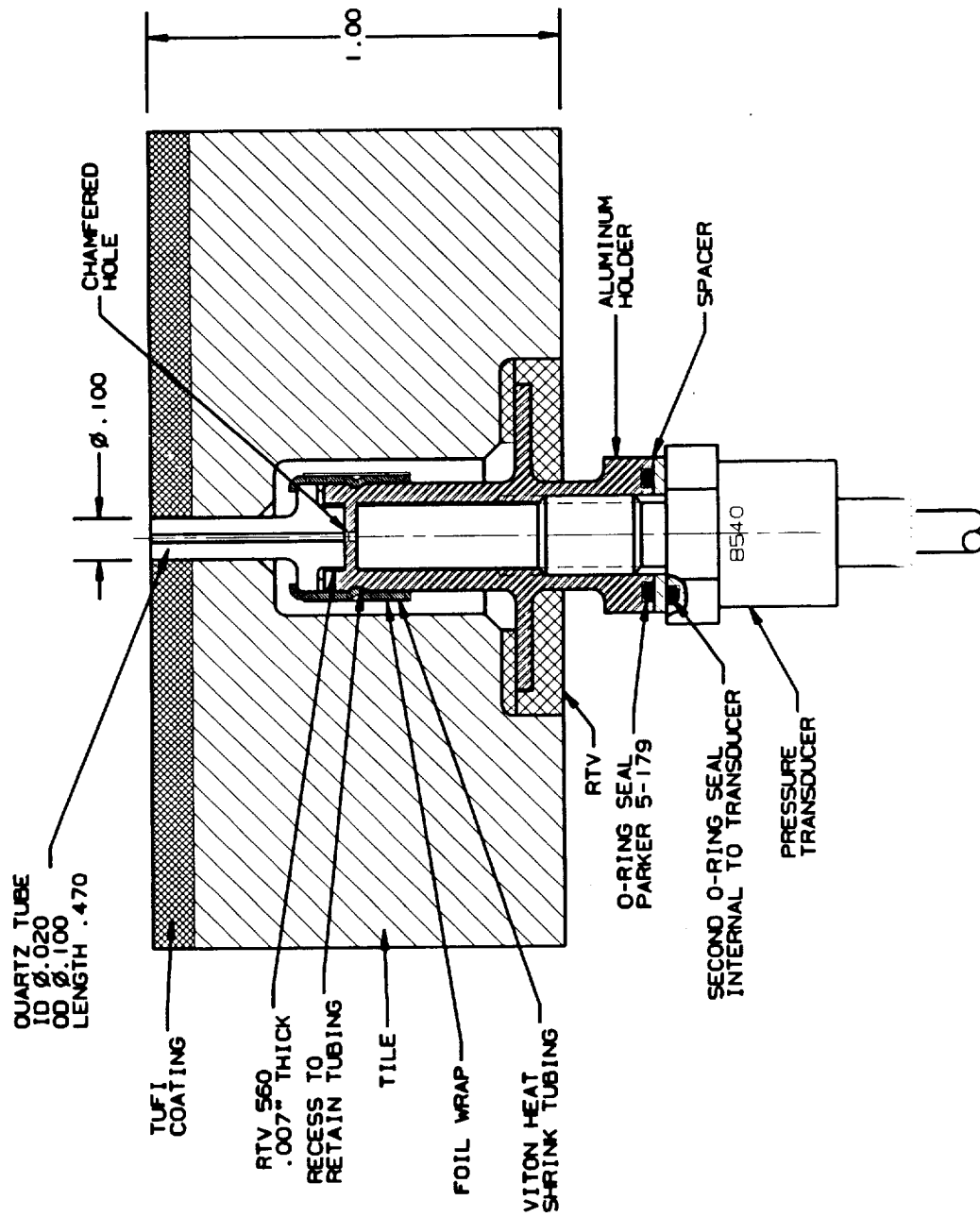


Figure 3. Final design of the Fixed Pressure Port.

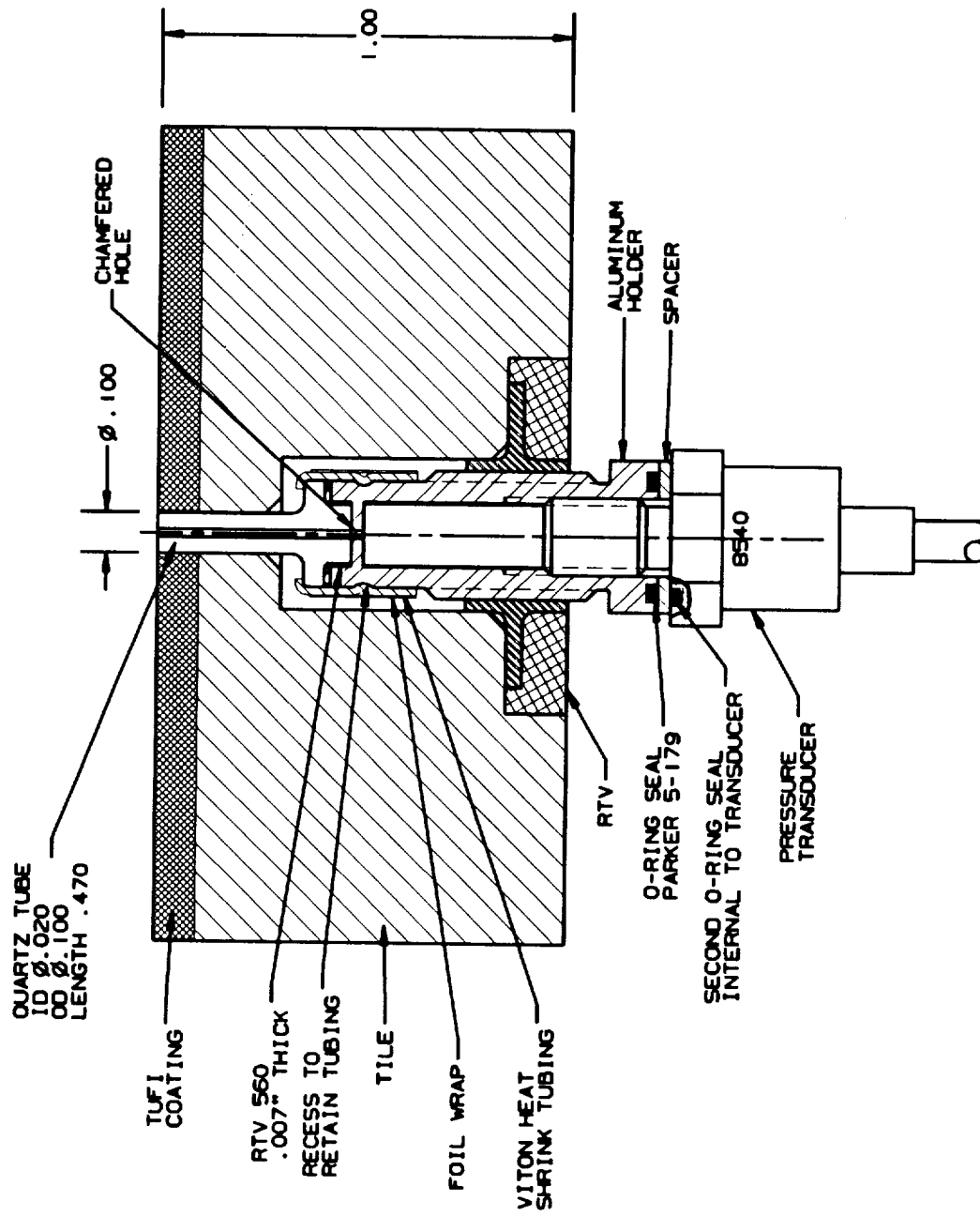


Figure 4. Final design of the Adjustable Pressure Port.



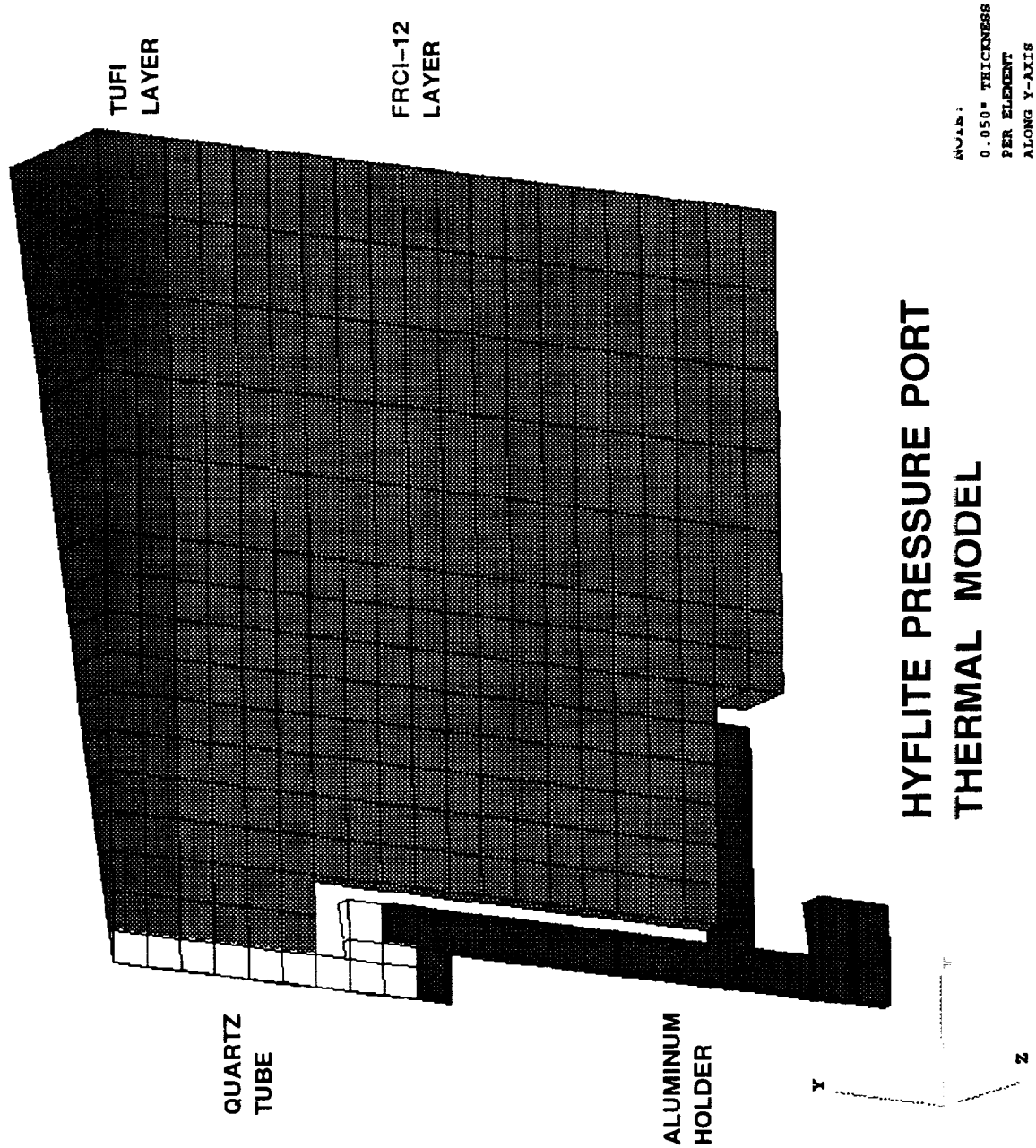


Figure 3. HYFLITE Pressure Port thermal model.

# HYFLITE BLT14H

## ISENTROPIC RAMP HEATING

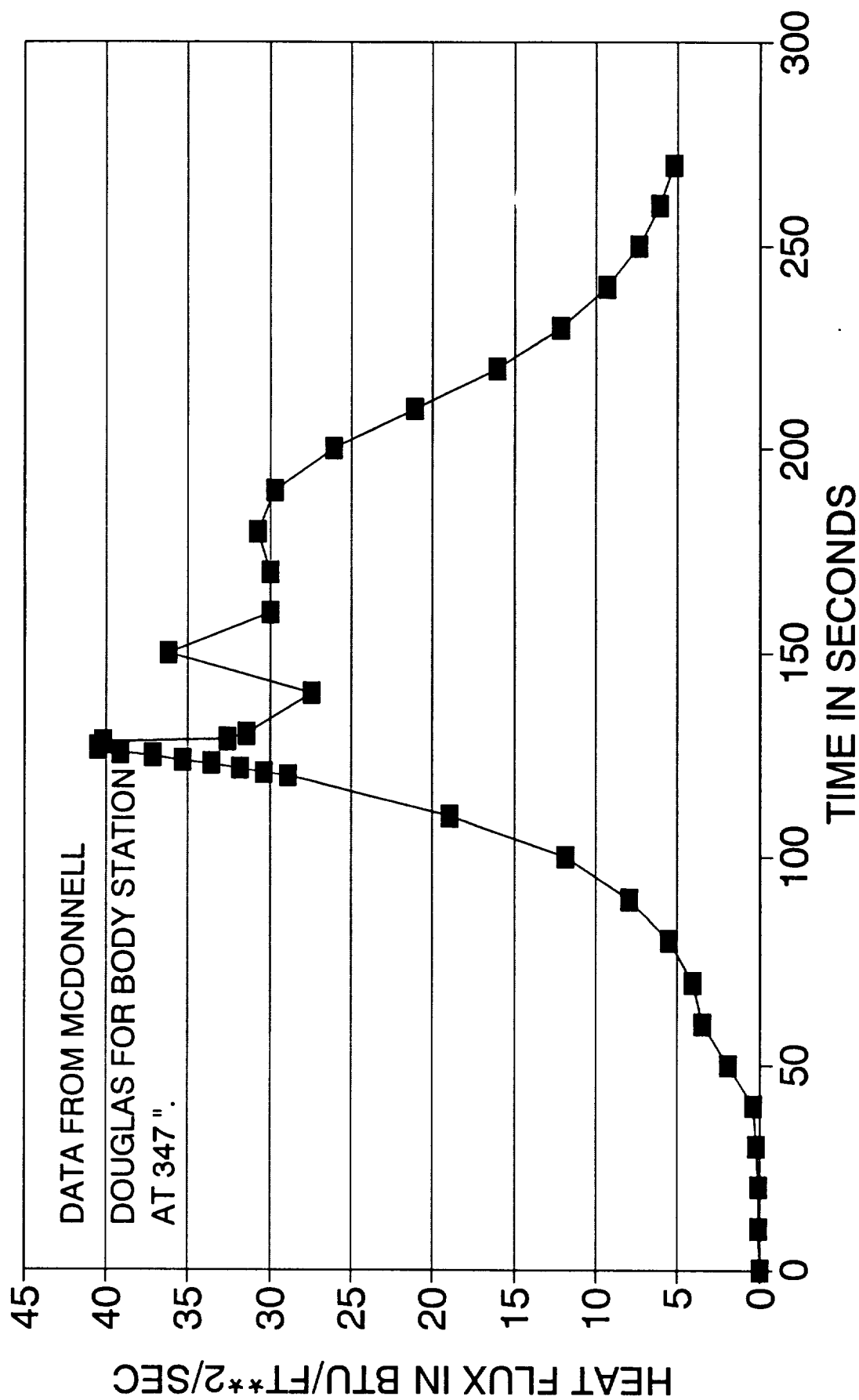
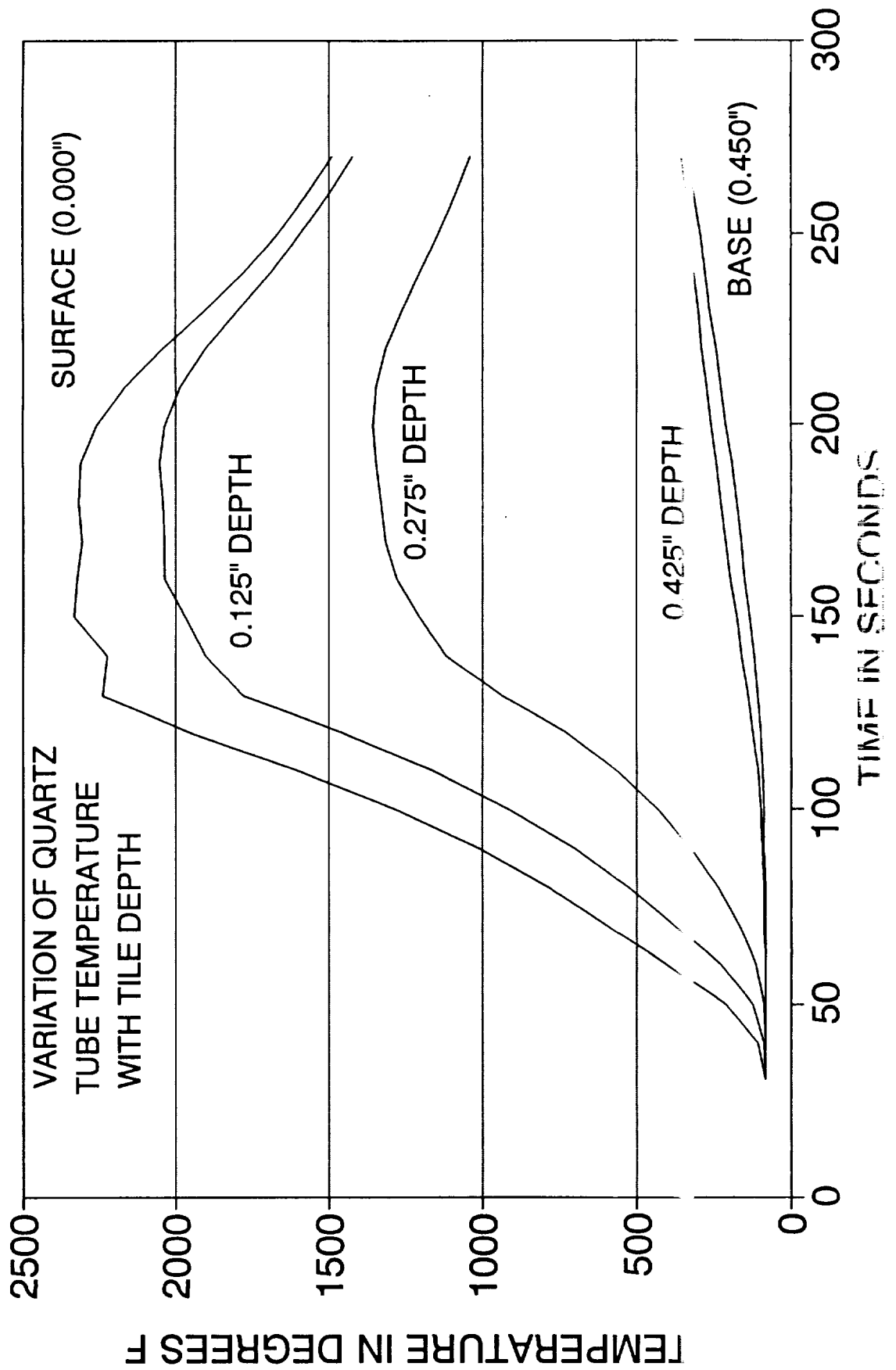


Figure 6. HYFLITE BLT14H Isentropic ramp heating.

# HYFLITE BLT14H

## PRESSURE PORT THERMAL MODEL



# HYFLITE BLT14H

## PRESSURE PORT THERMAL MODEL

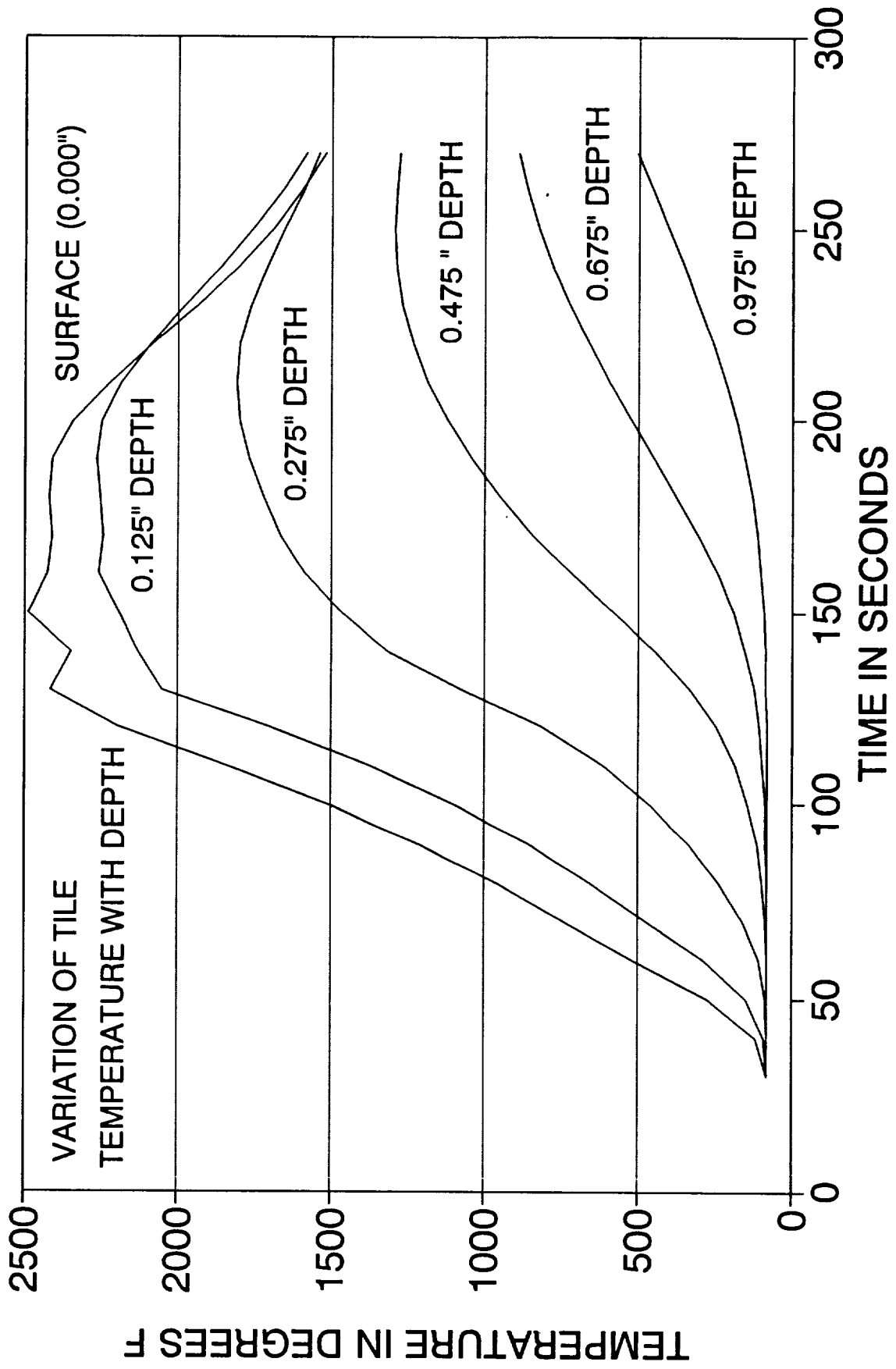
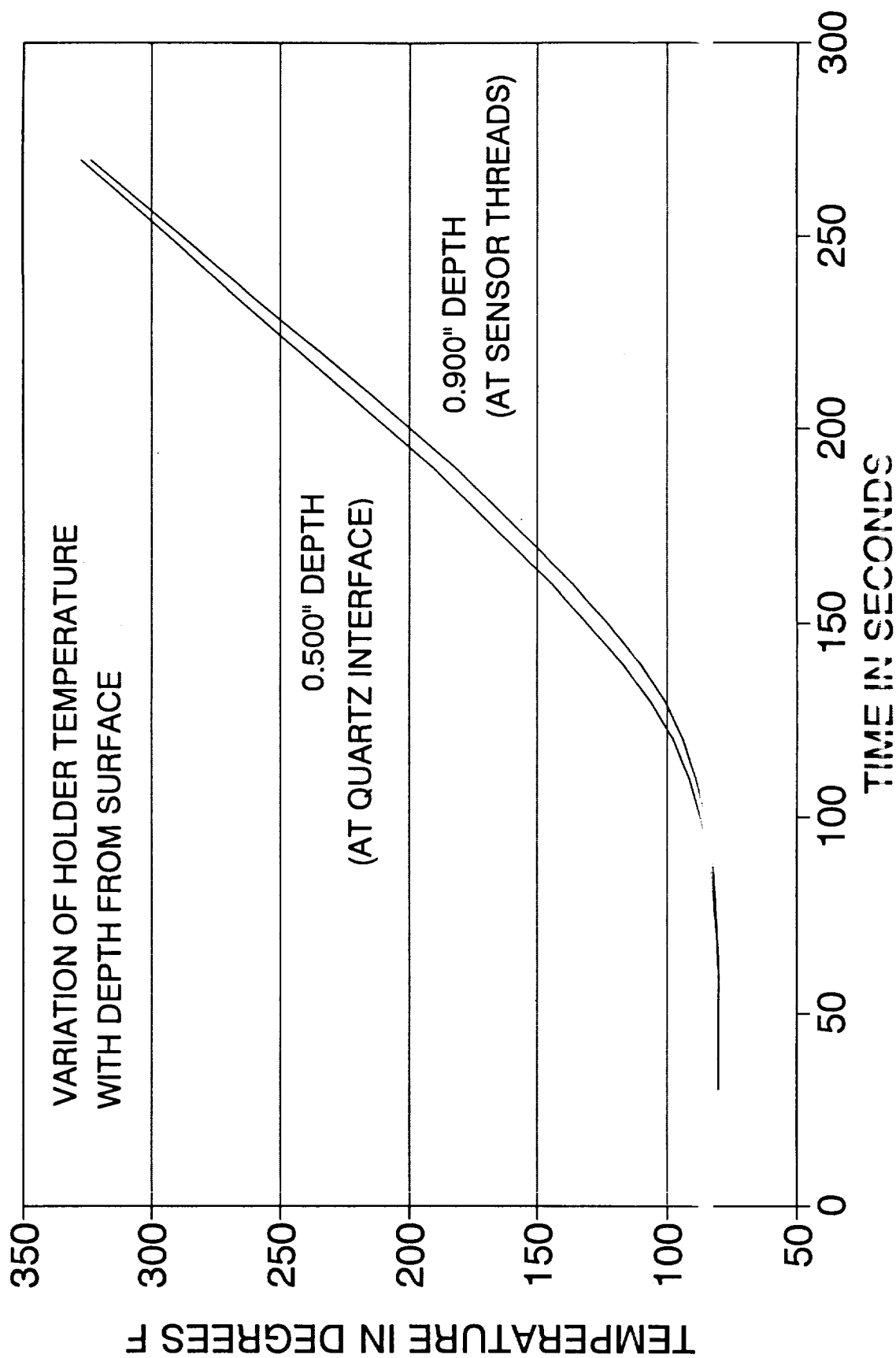


Figure 8. HYFLITE BLT14H - Variation of tile temperature with depth.

# HYFLITE BLT14H

## PRESSURE PORT THERMAL MODEL



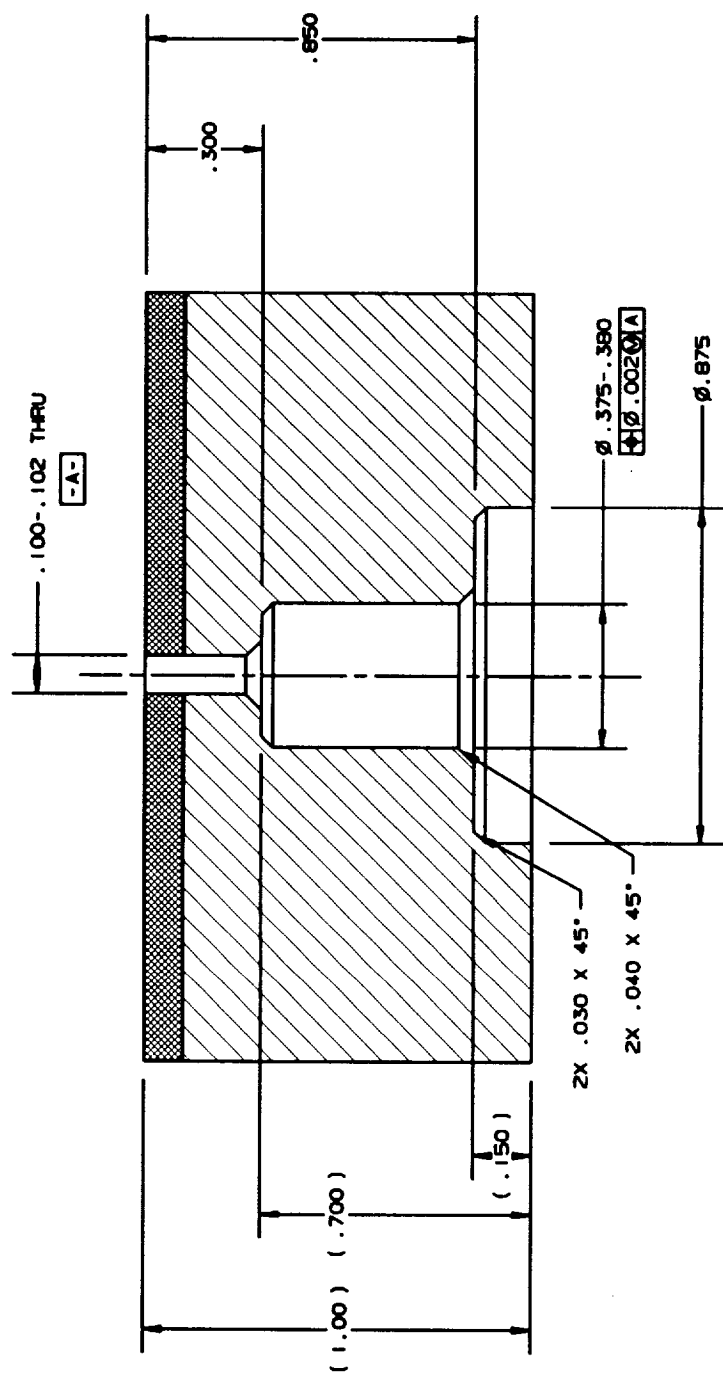


Figure 10. Tile core detail.

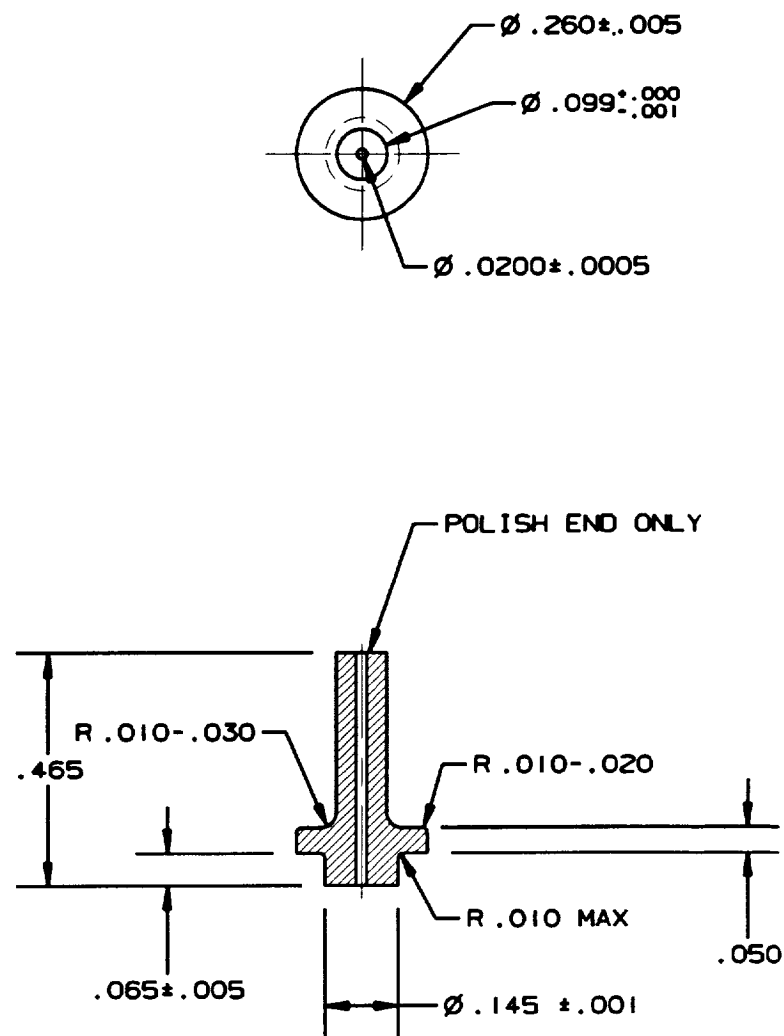


Figure 11. Drawing of the quartz tube.

# RANDOM VIBRATION TEST SPECTRUM FOR HYFLITE SPECIMEN

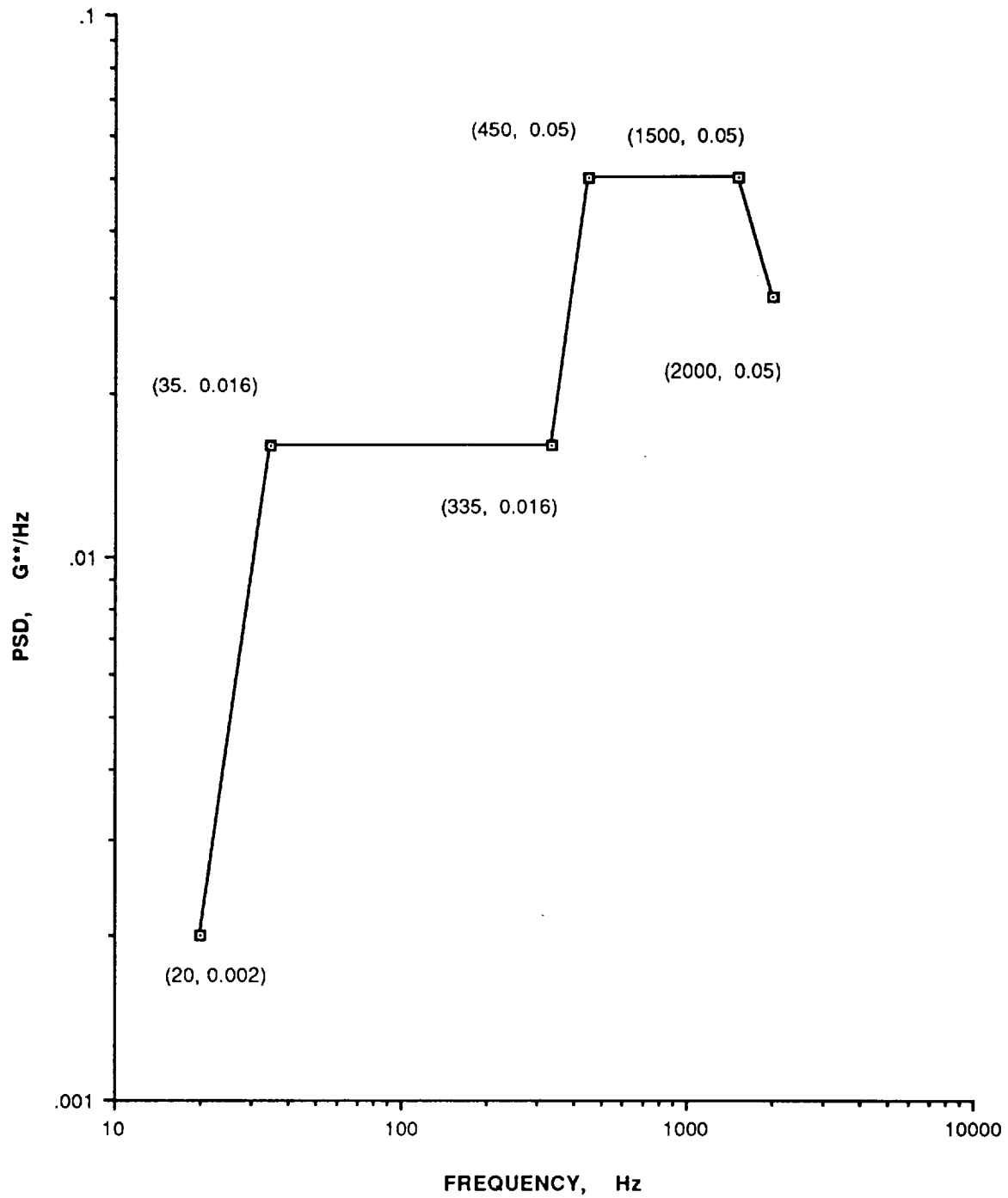


Figure 12. Random vibration test spectrum for HYFLITE specimen.



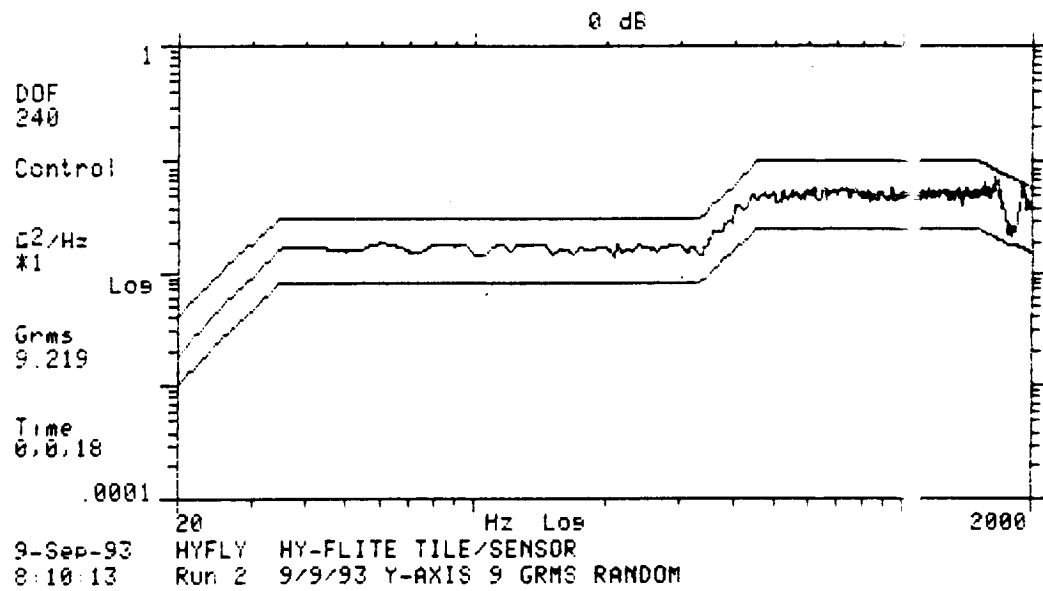


Figure 13. Vibration test input spectrum.

## Temperature Profile

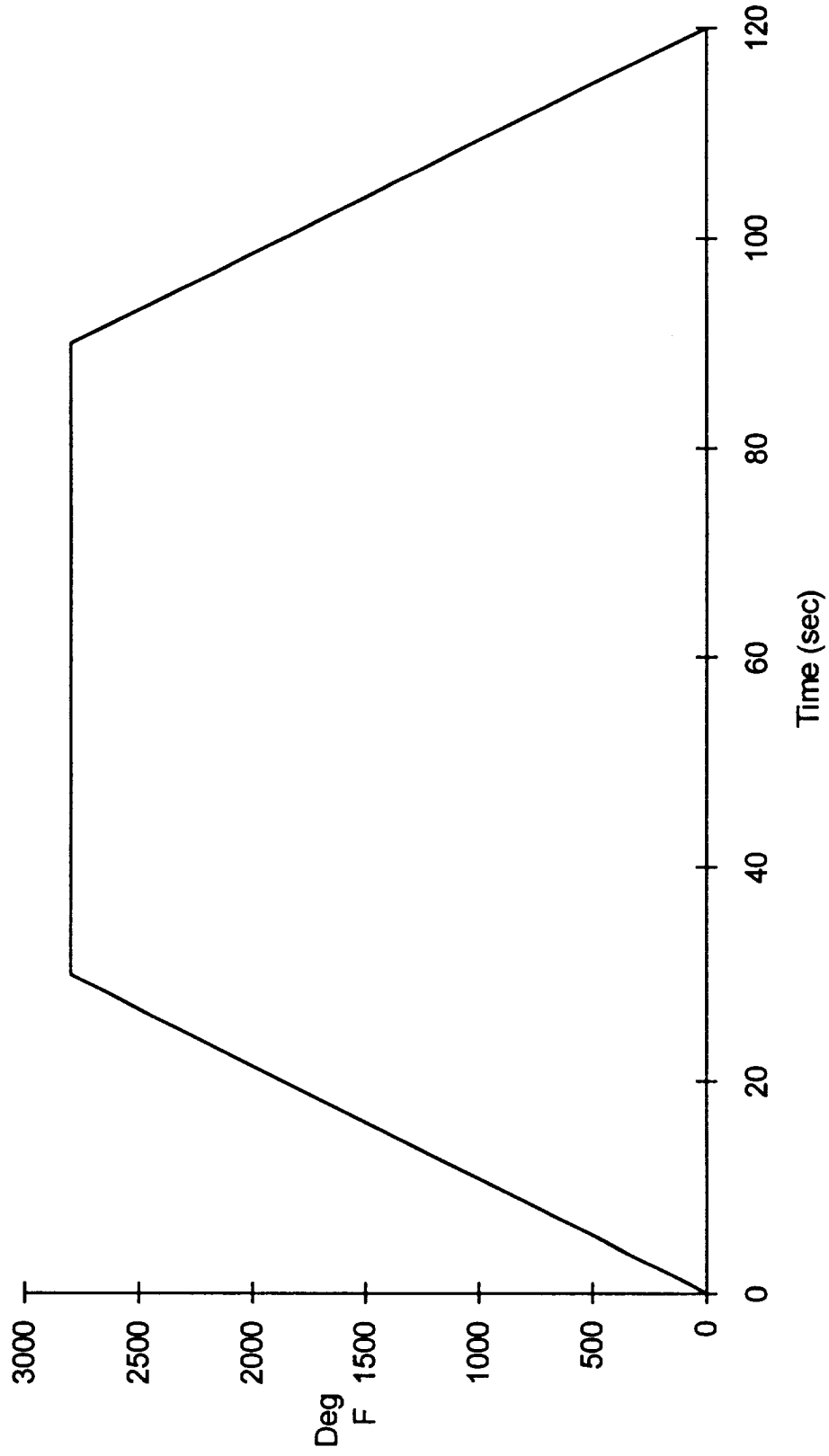


Figure 14. Desired aero-thermal test temperature profile.

# AMES 2 X 9 DUCT FACILITY

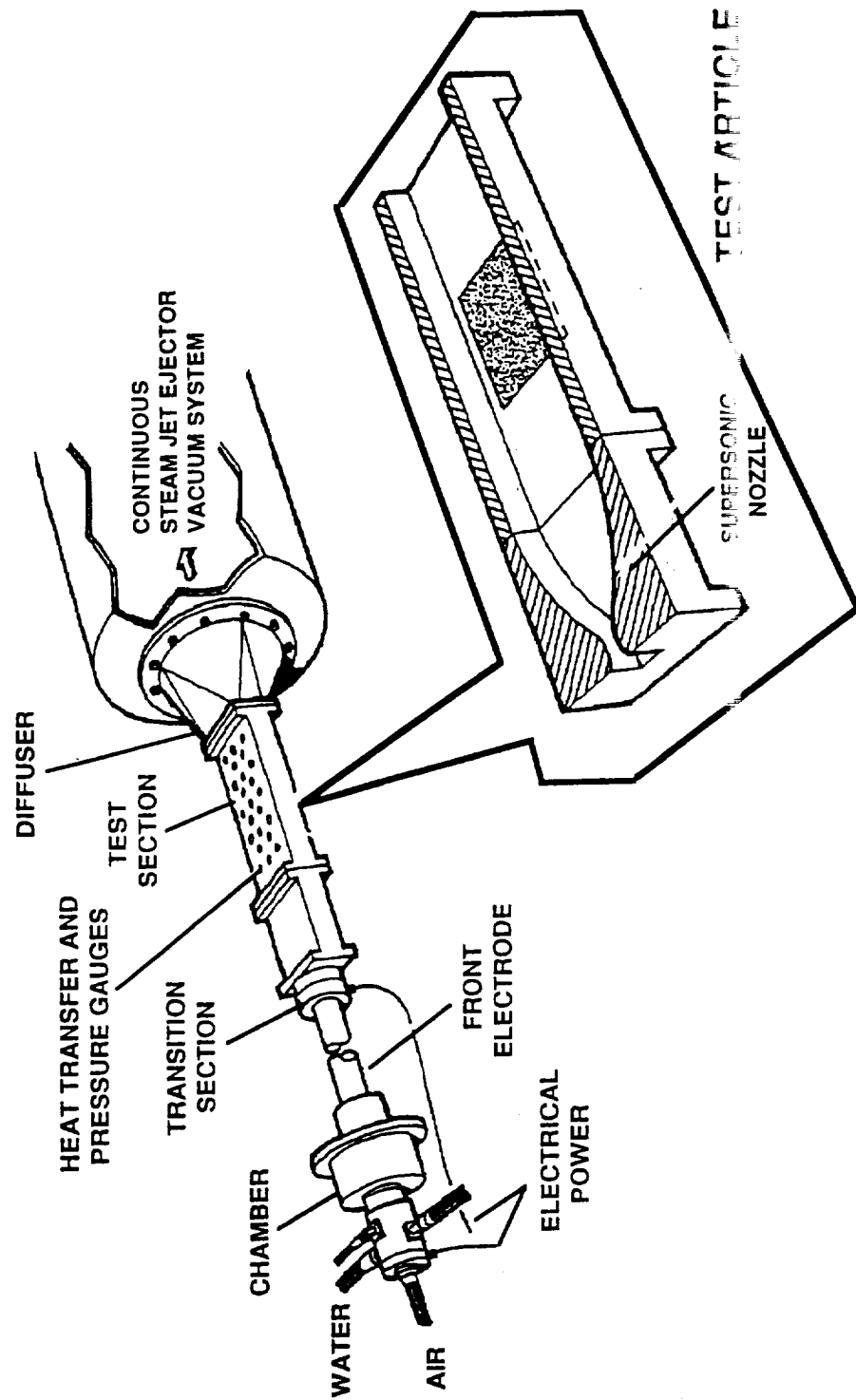


Figure 15. Ames 2 x 9 Turbulent Flow Duct Facility



Figure 16. Aerial view of Thermophysics Test Facility.

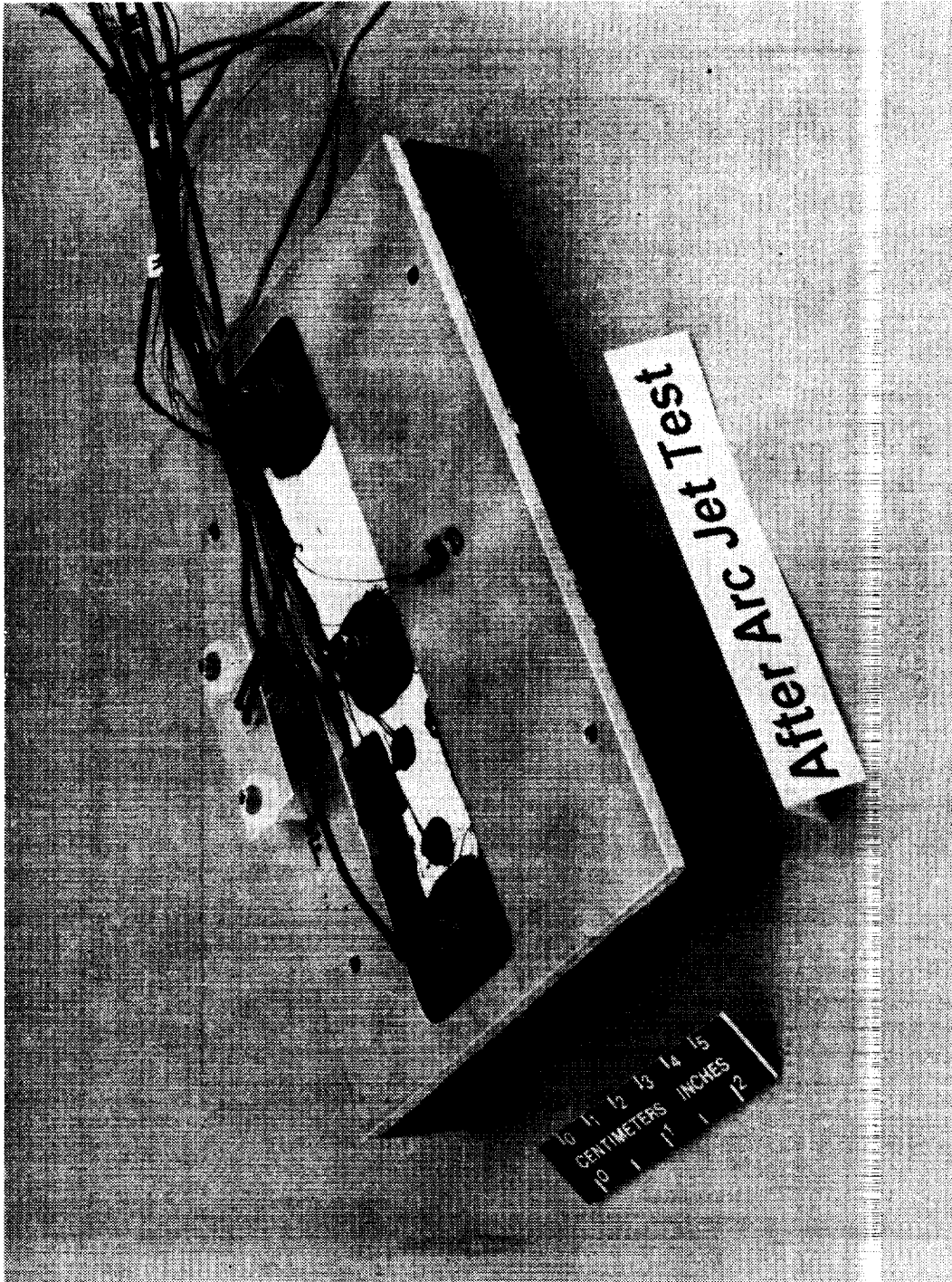


Figure 17. Isometric view of test specimen.

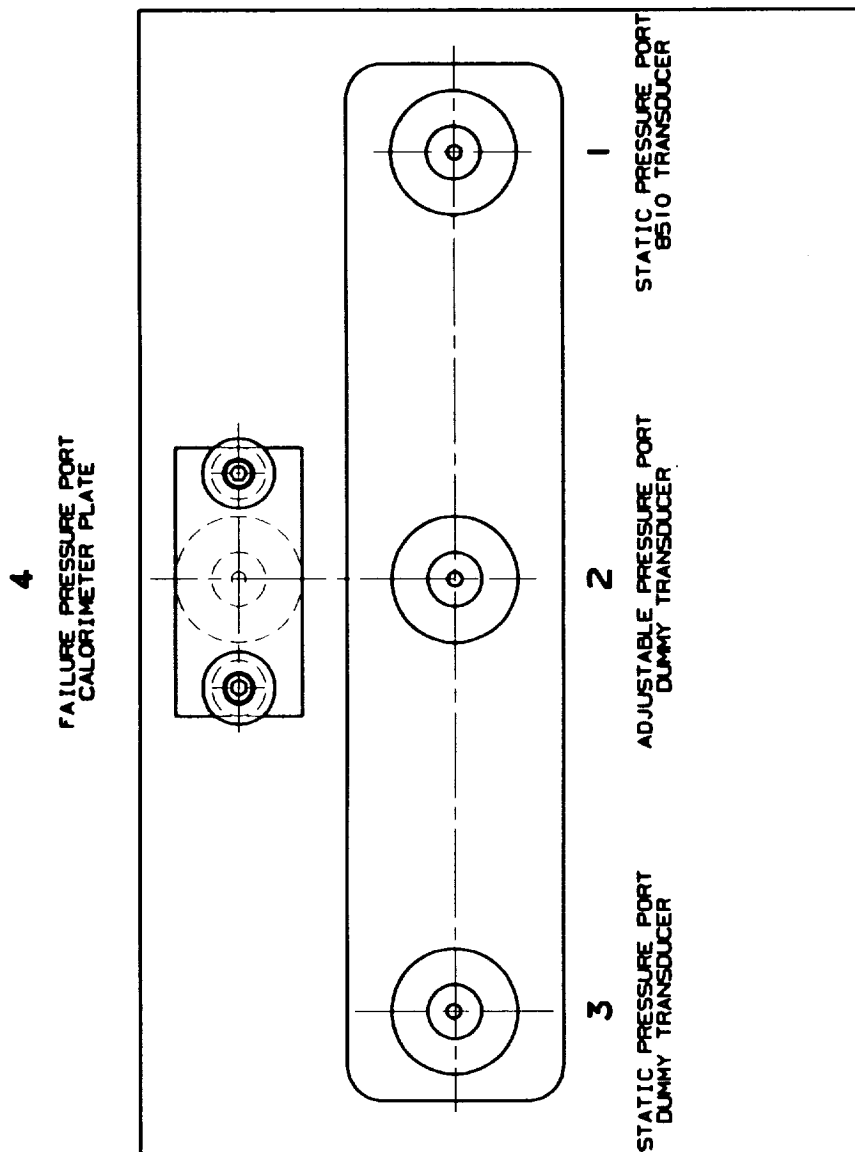


Figure 18. Schematic bottom view of the test specimen.

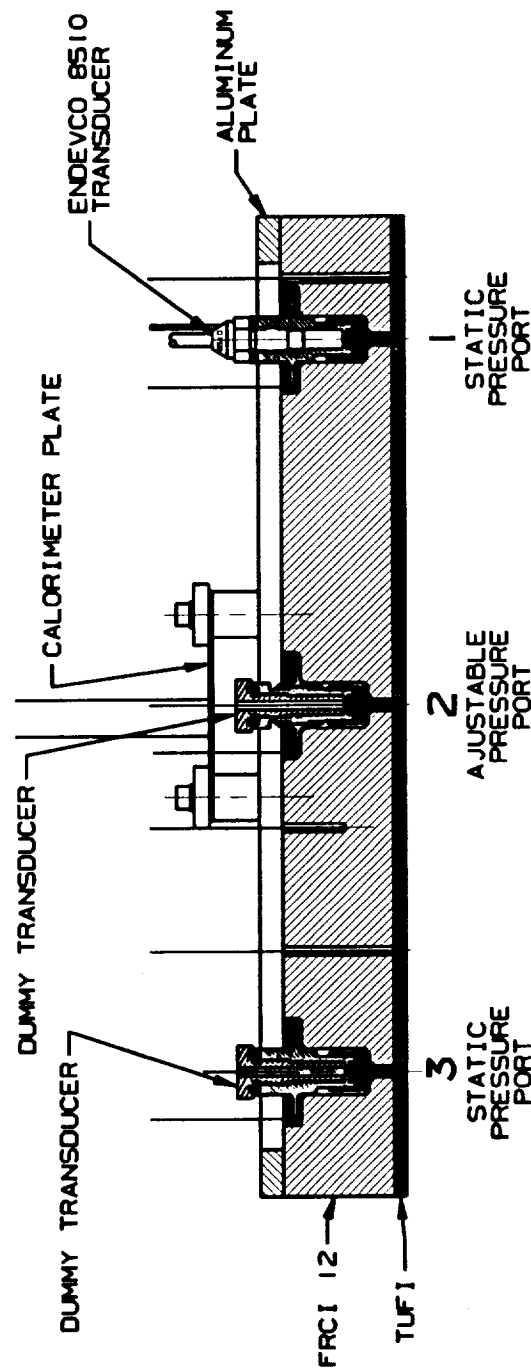


Figure 19. Schematic cross section of test specimen.

# HYFLITE Test Article Layout

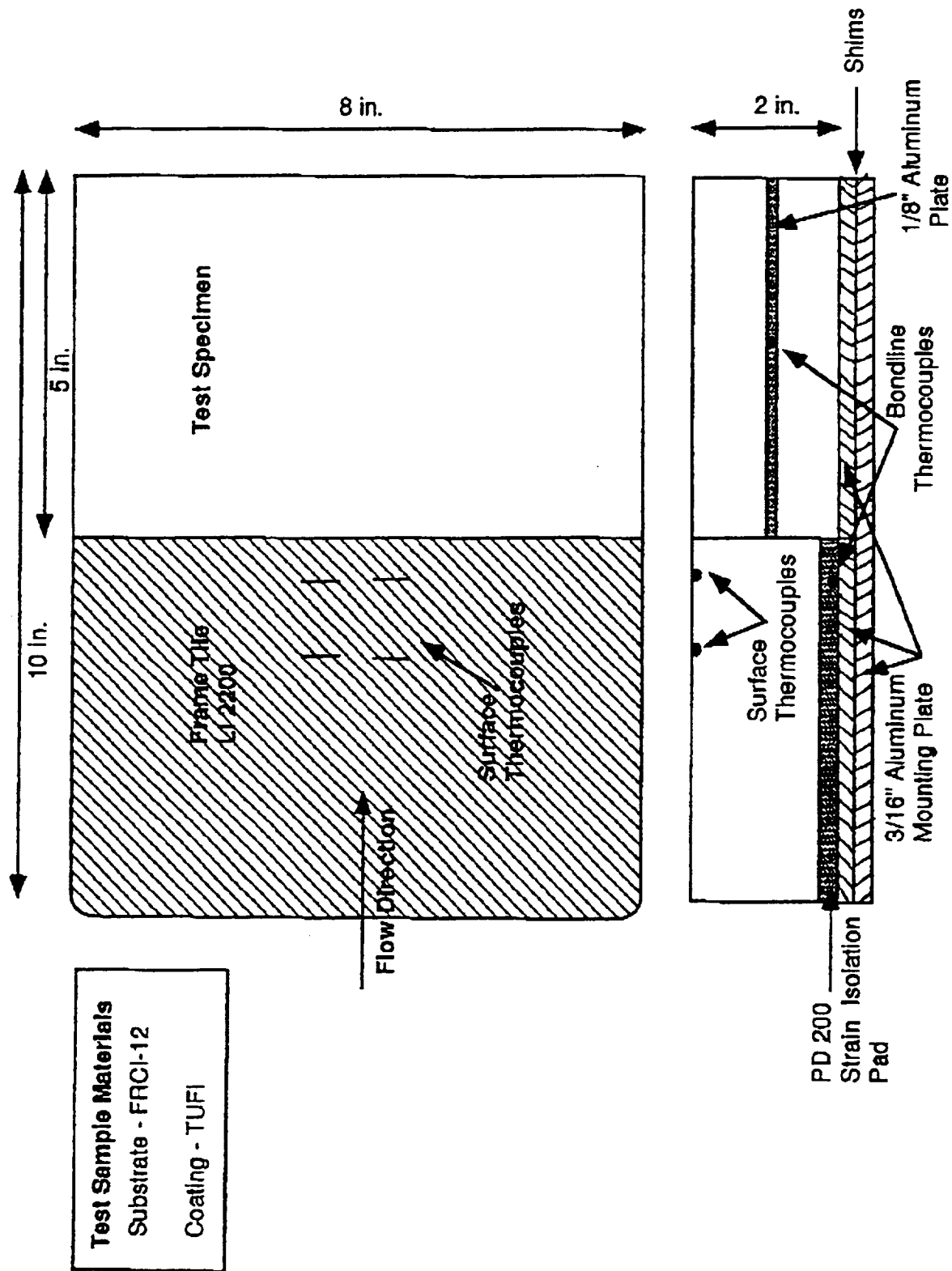


Figure 20. HYFLITE test article layout.



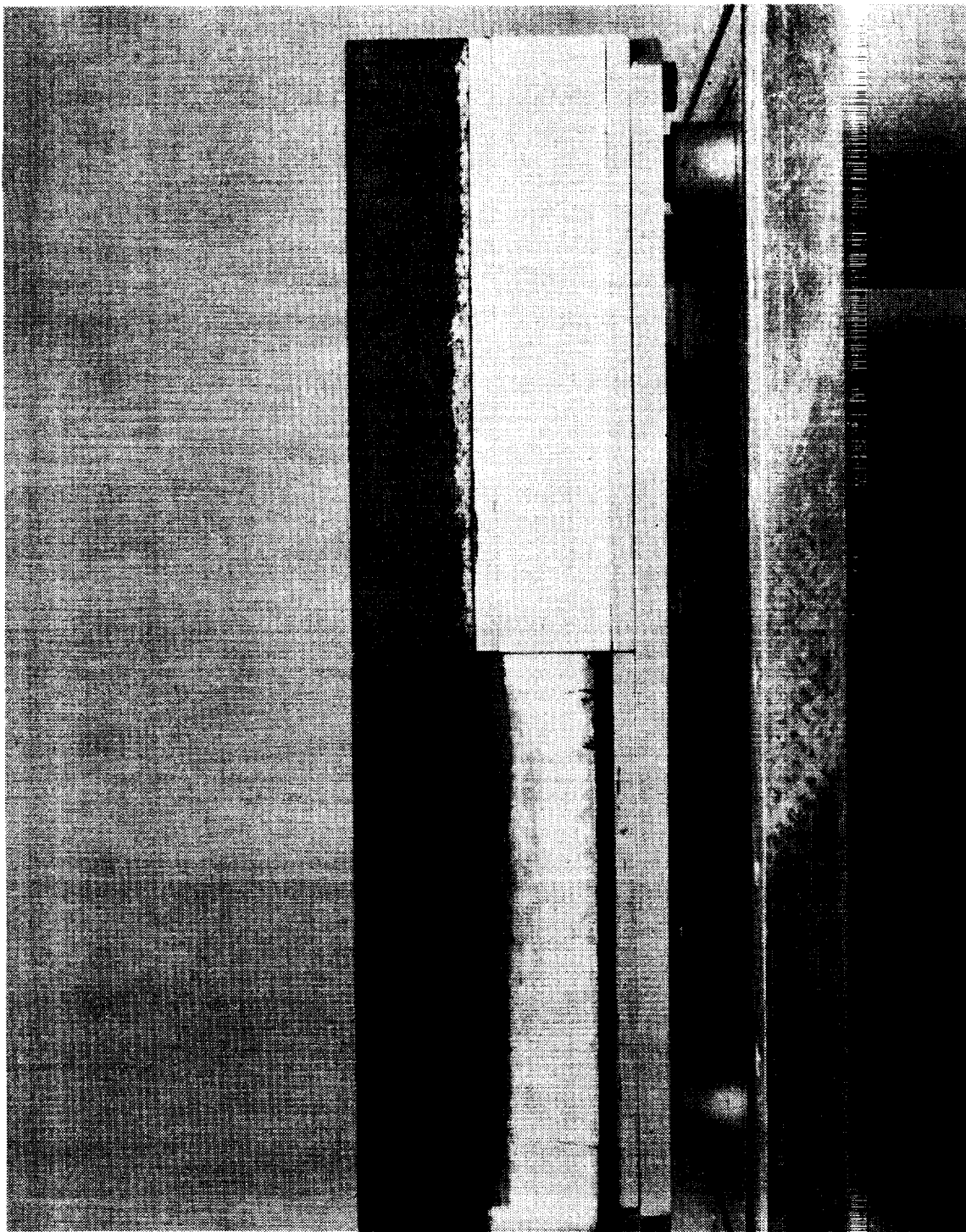


Figure 21. Side view of test assembly prior to aero-thermal test.

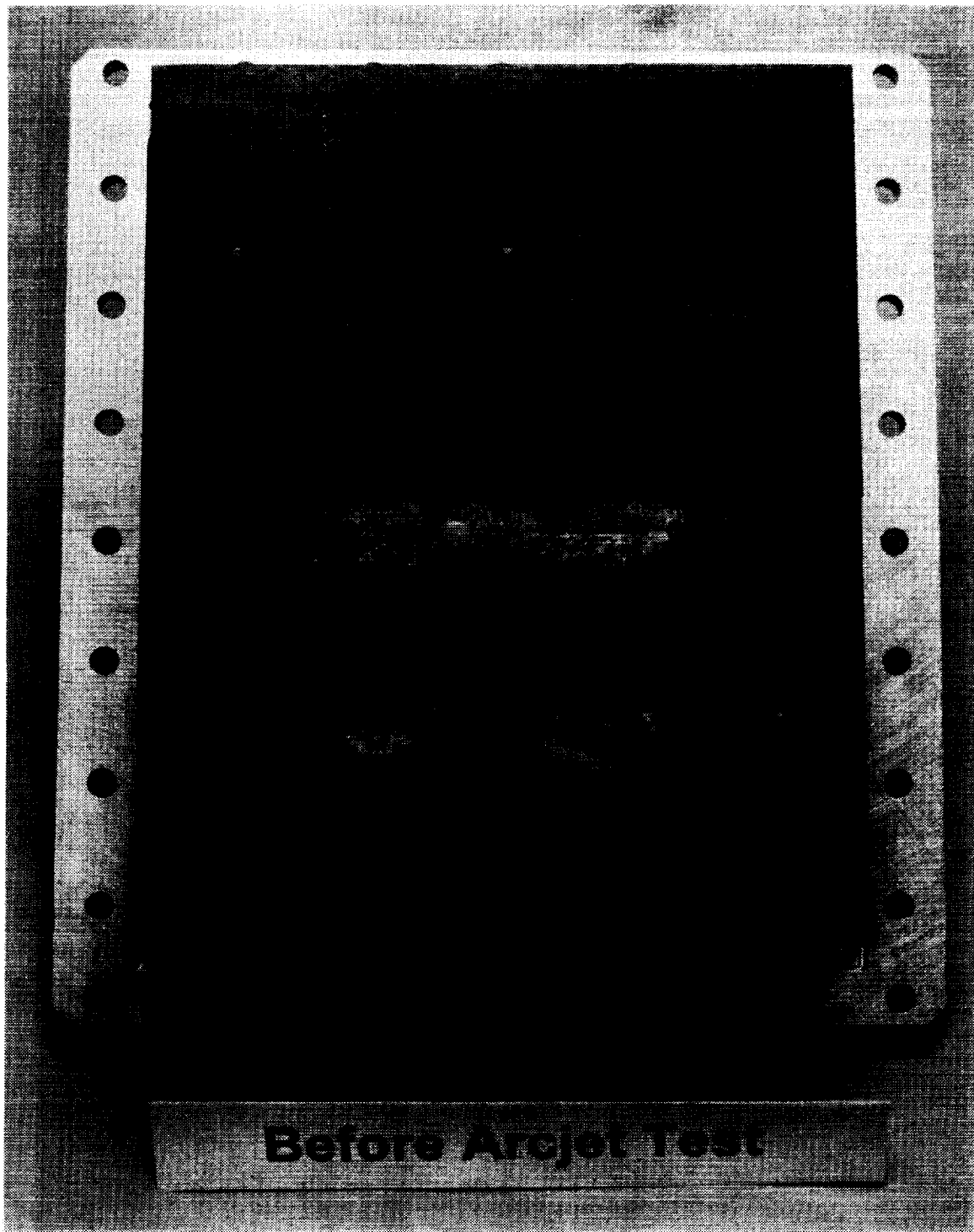
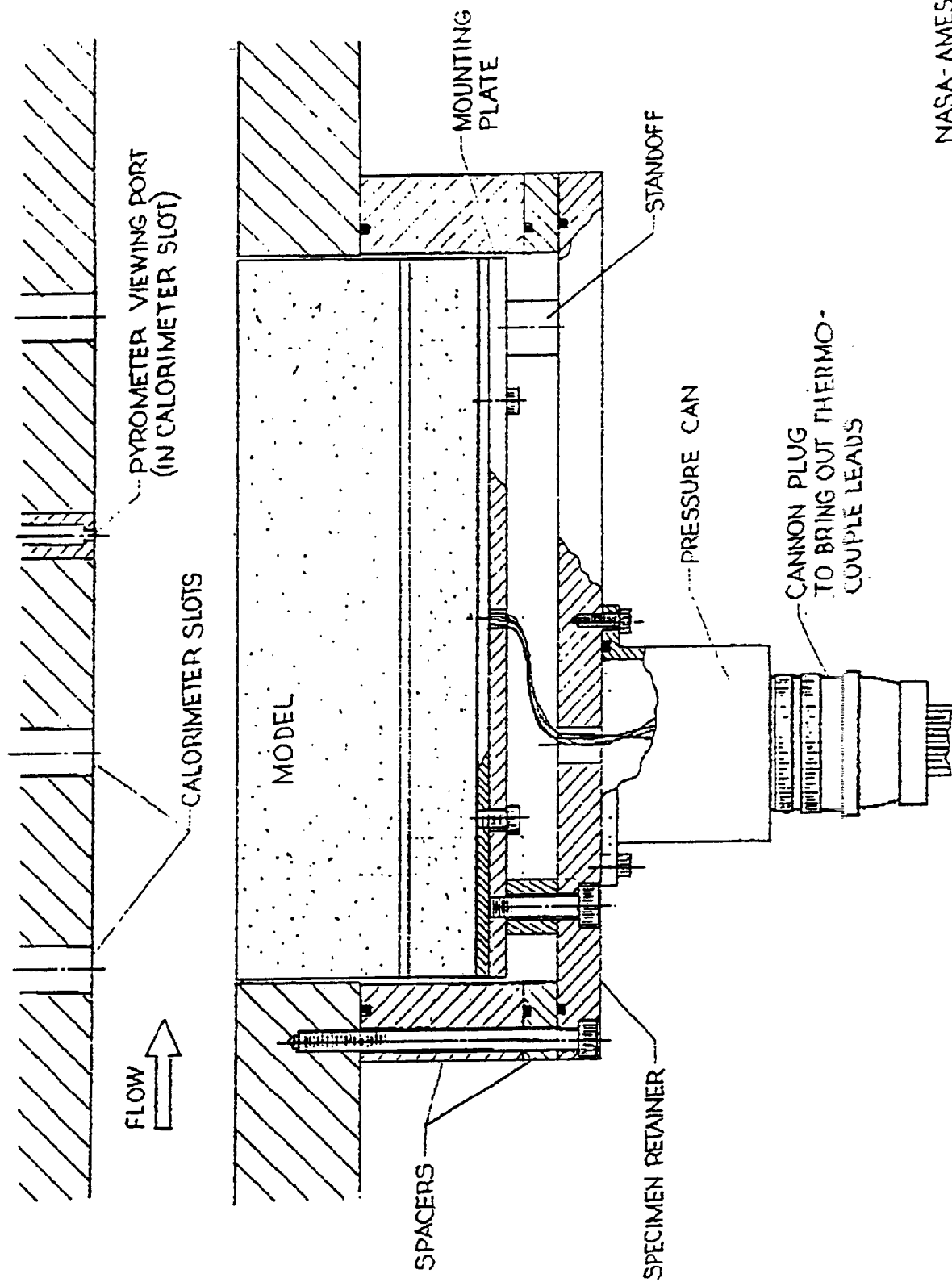


Figure 22. Top view of test assembly prior to aero-thermal test.



NASA-AMES  
MARCH 1984

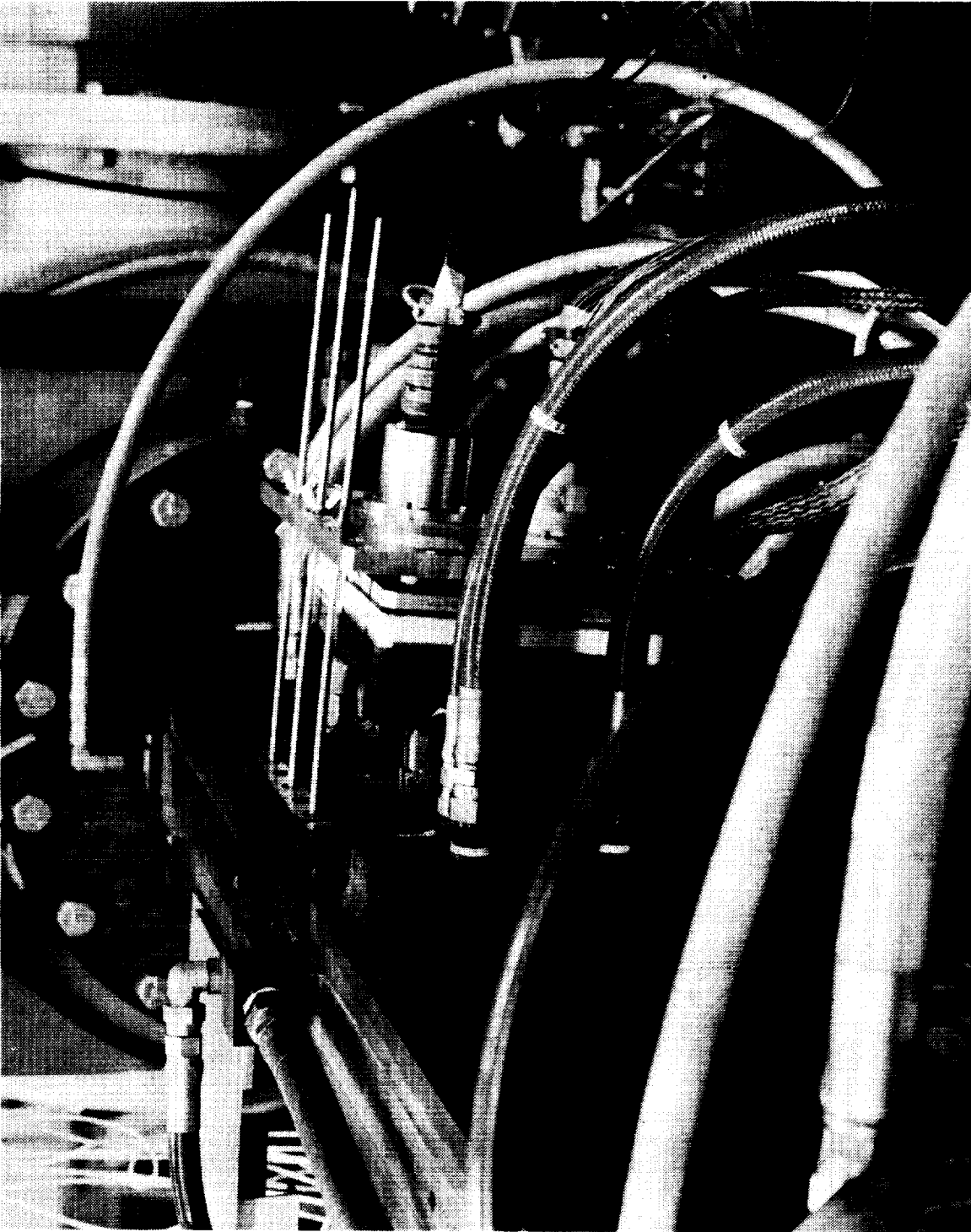


Figure 24. Test assembly during calibration run.

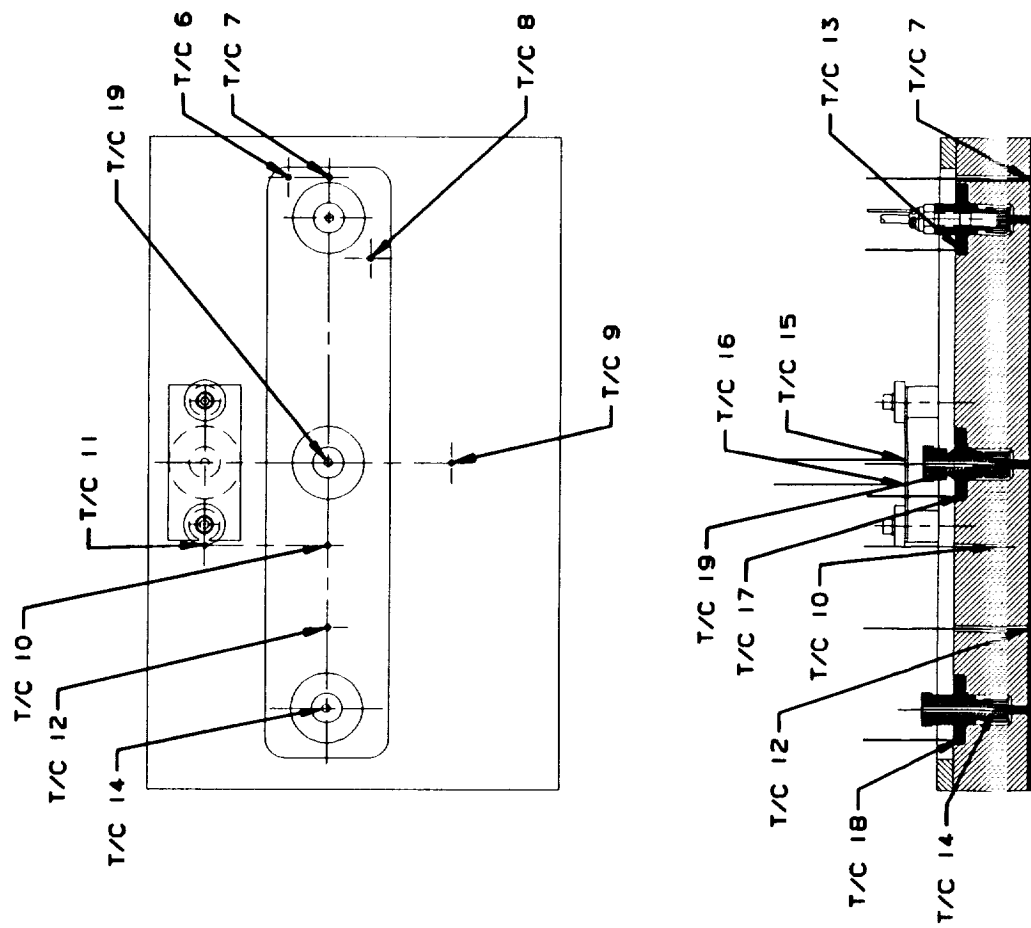
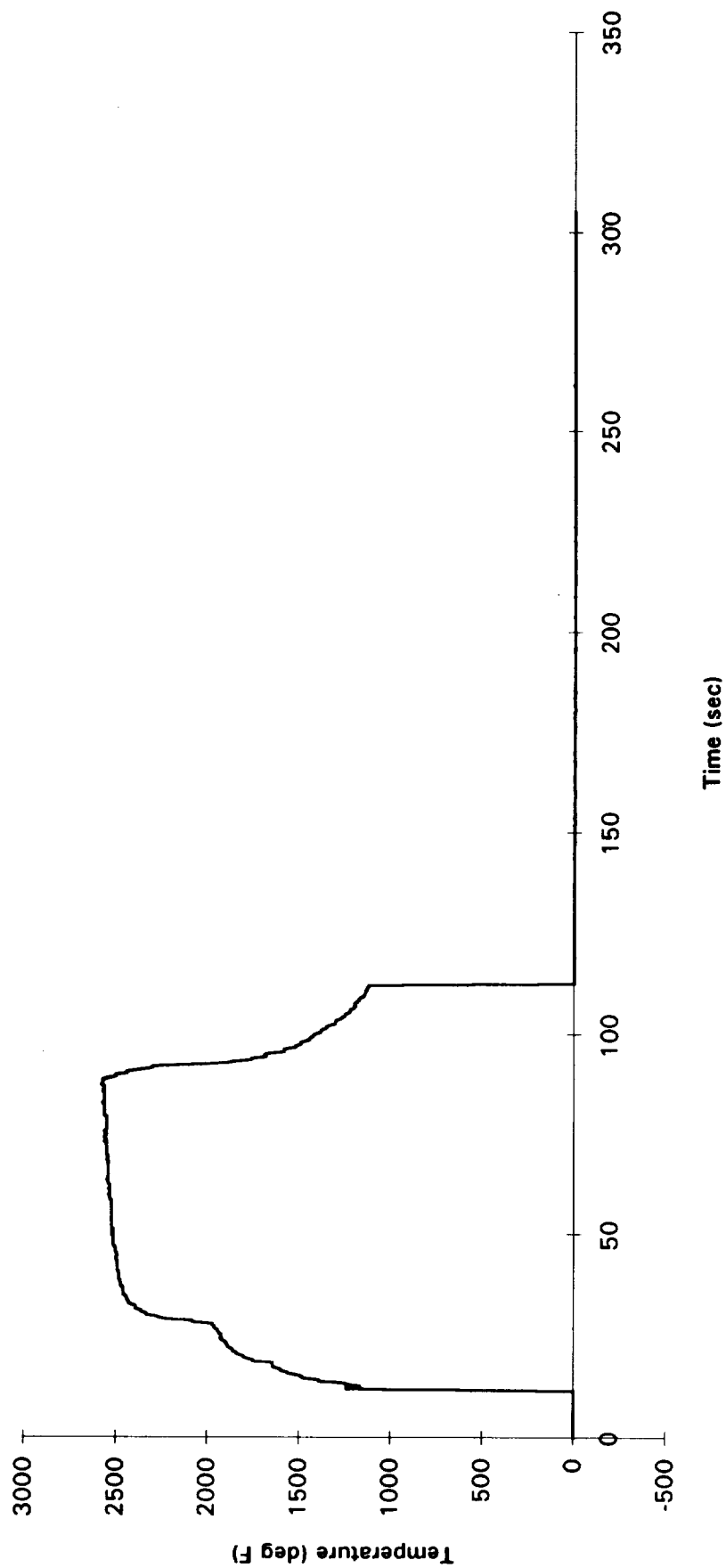


Figure 25. Tile thermocouple locations.

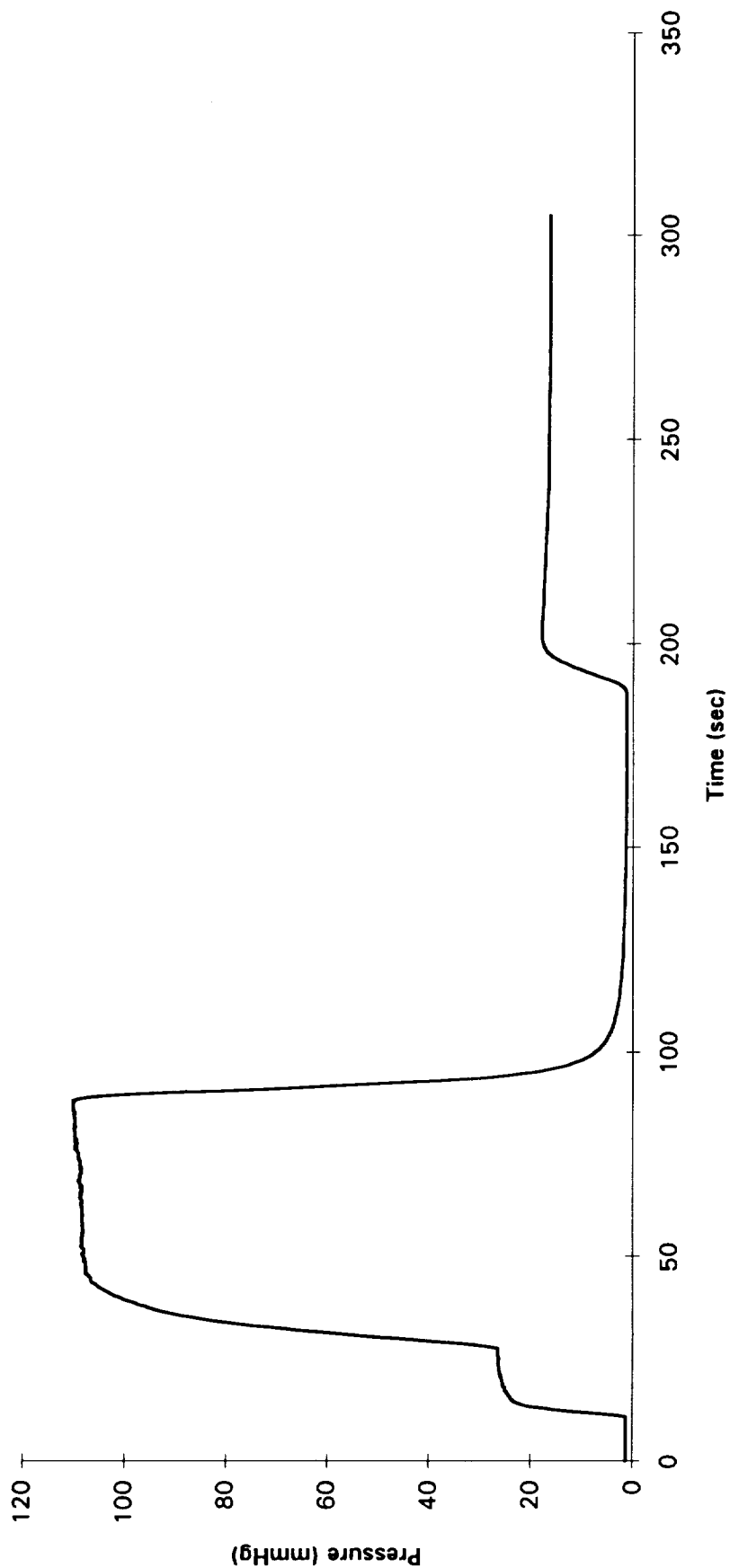
## Pyrometer



Ames 2X9 Arc Jet  
10/7/93

Figure 26. Plot of pyrometer data, pyrometer located on the opposite wall of the test chamber.

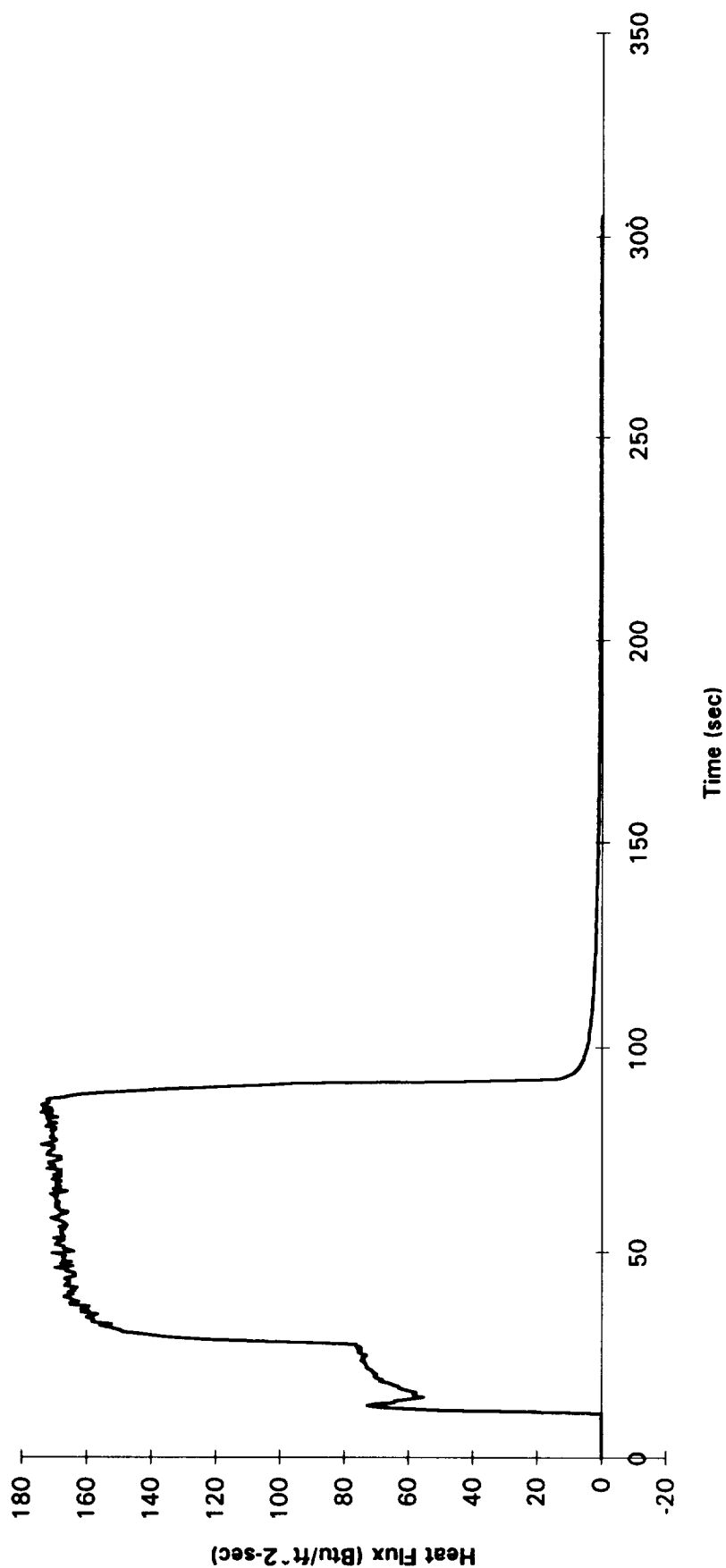
# Average Pressure



Ames 2X9 Arc Jet  
10/7/93

Figure 27. Plot of average chamber pressure, sensors located on the opposite wall of the test chamber.

# Average Heat Flux

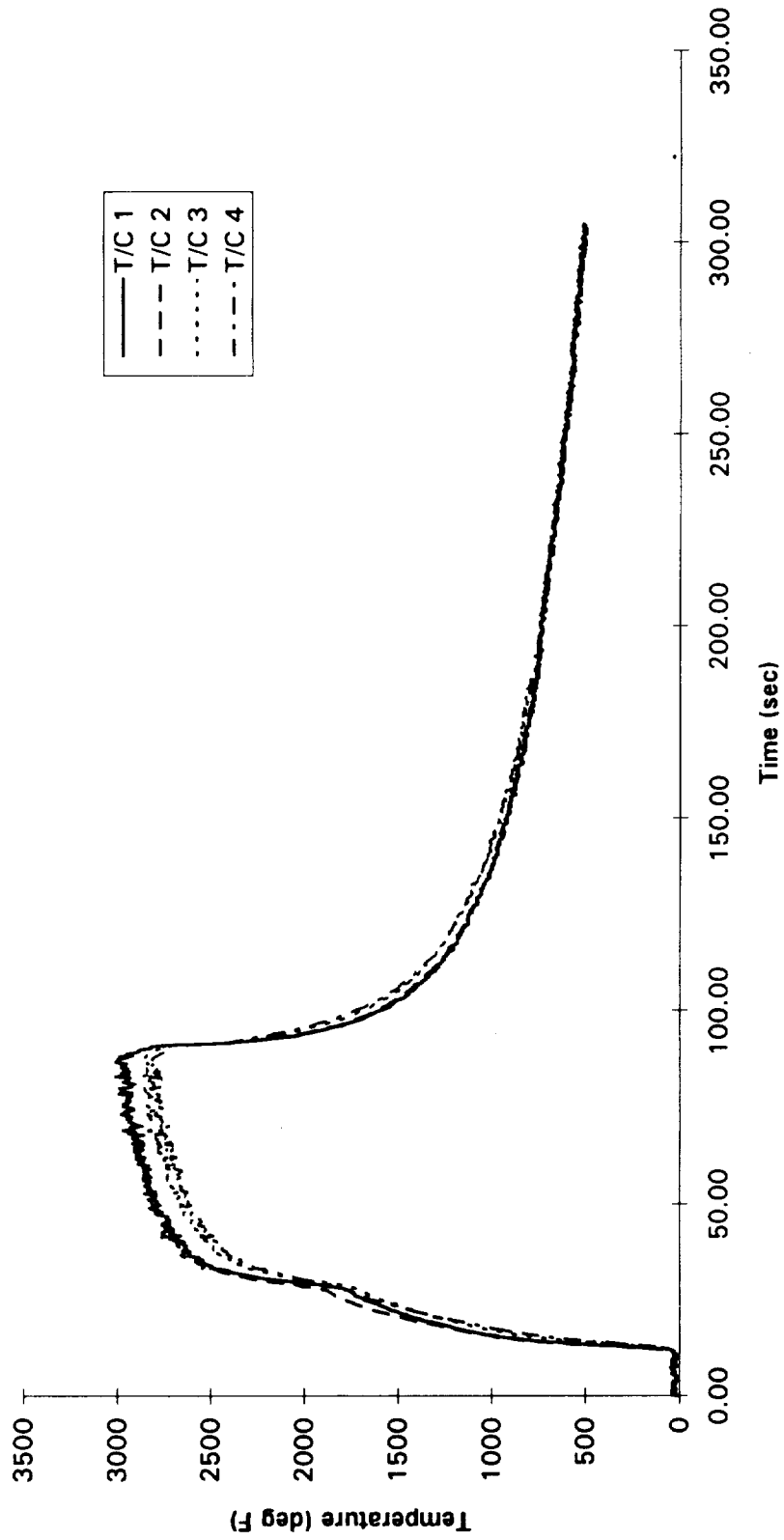


Ames 2X9 Arc Jet  
10/7/93

Figure 28. Plot of chamber heat flux, calorimeters located on the opposite wall of the test chamber.



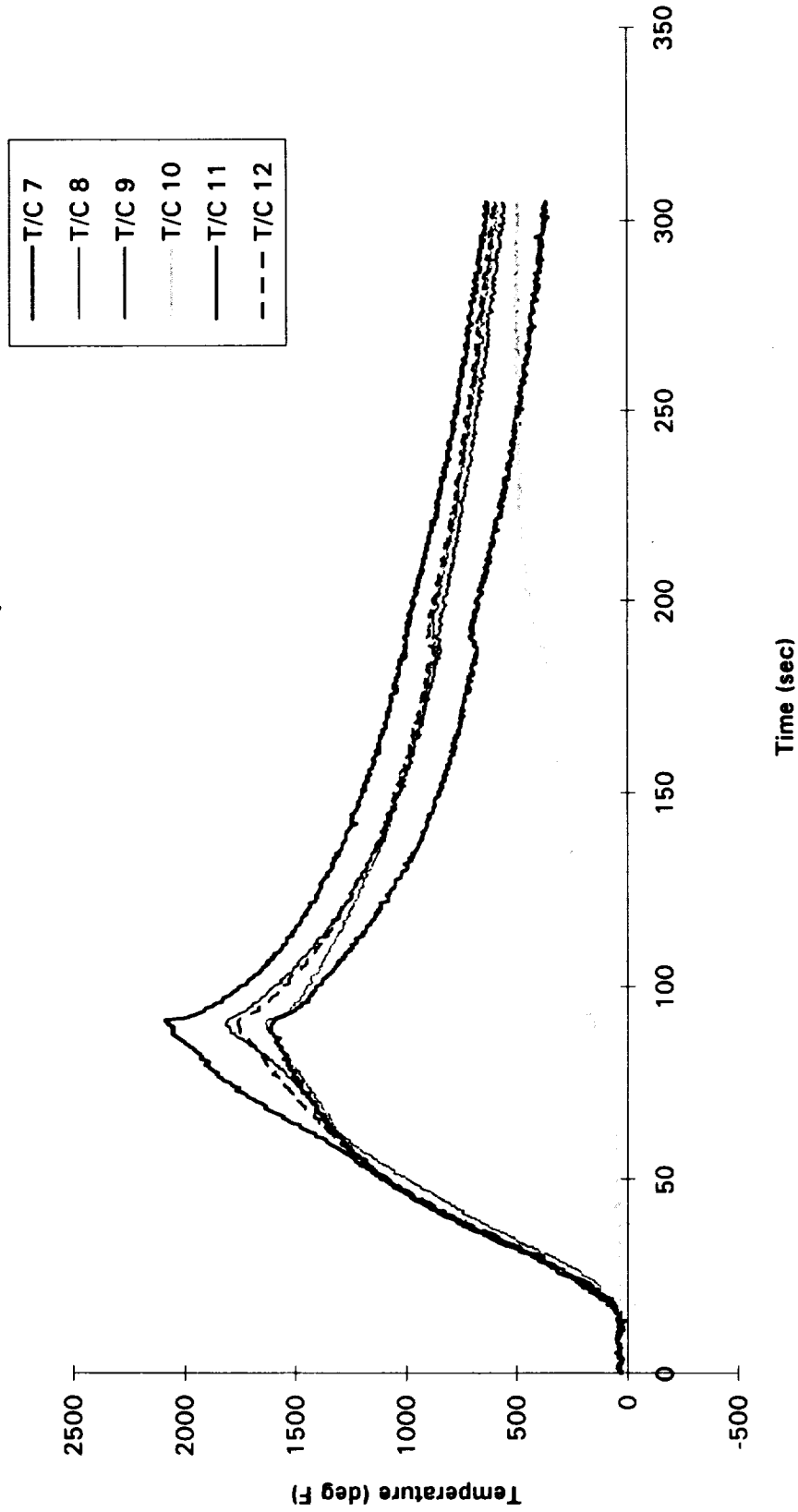
# Surface Thermocouples



ANALYSIS DATE: 10/7/93

Figure 29. Plot of surface thermocouples, thermocouples located upwind of test specimen.

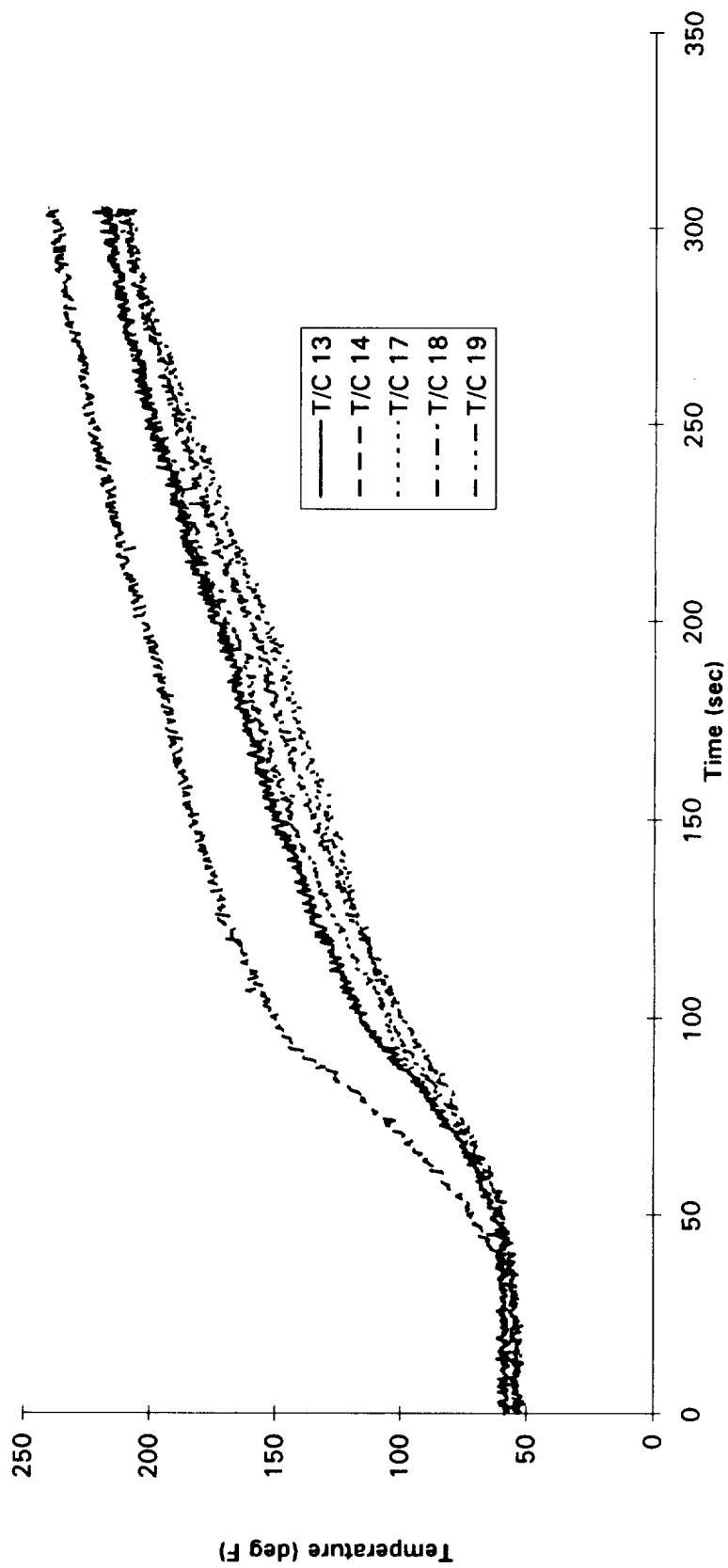
# Tile Thermocouples



Ames 2X9 Arc Jet  
10/7/93

Figure 30. Plot of tile thermocouple temperatures, thermocouples located .1 inch from tile surface except T/C located .5 inch from tile surface.

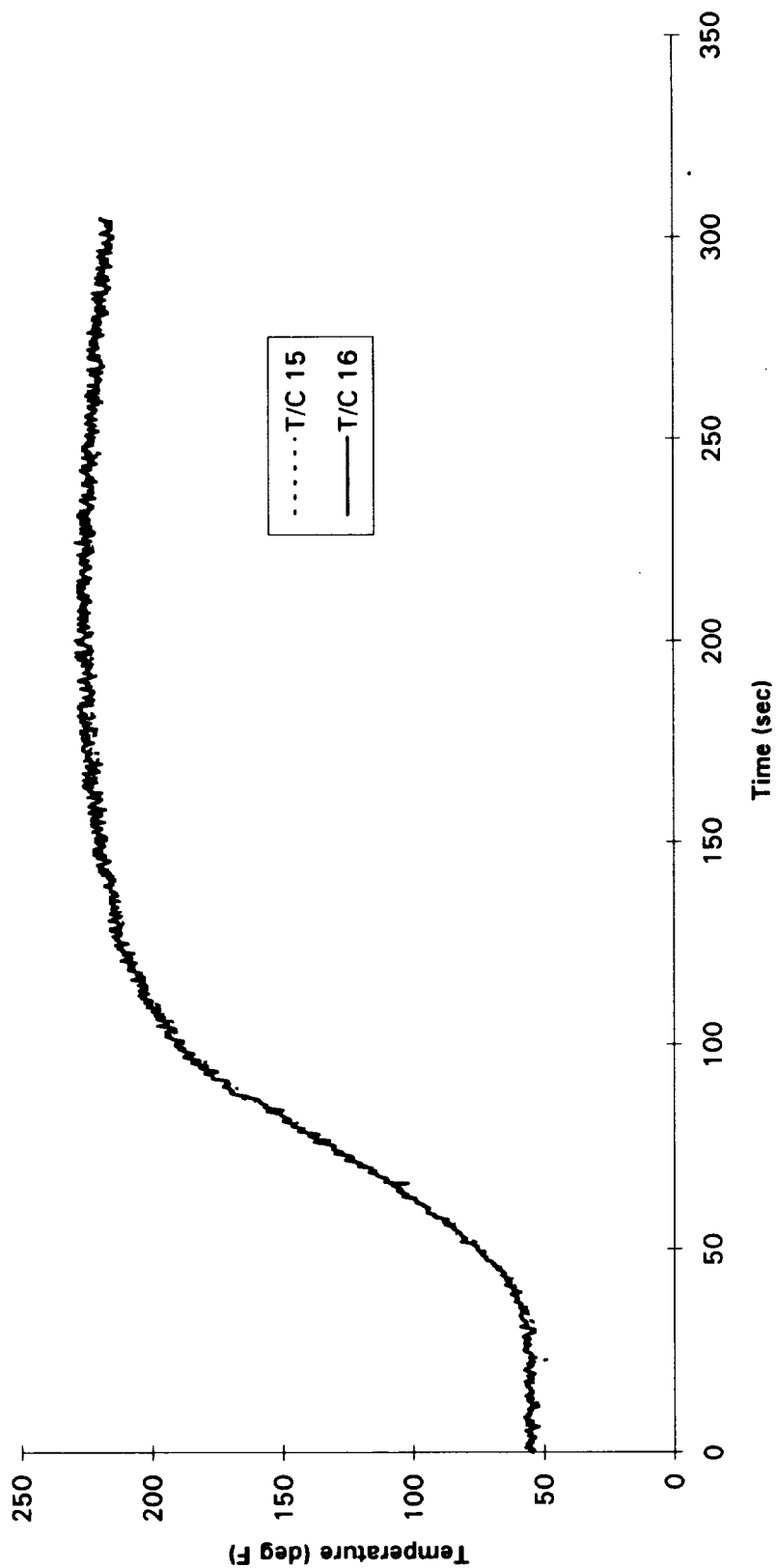
# Pressure Port Thermocouples



Run 248 Air Jet  
10/7/93

Figure 31. Plot of pressure port thermocouple temperatures.

# Calorimeter Plate Thermocouples



Ames 2X9 Arc Jet  
10/7/93

Figure 32. Plot of site #4 calorimeter plate thermocouple temperatures.

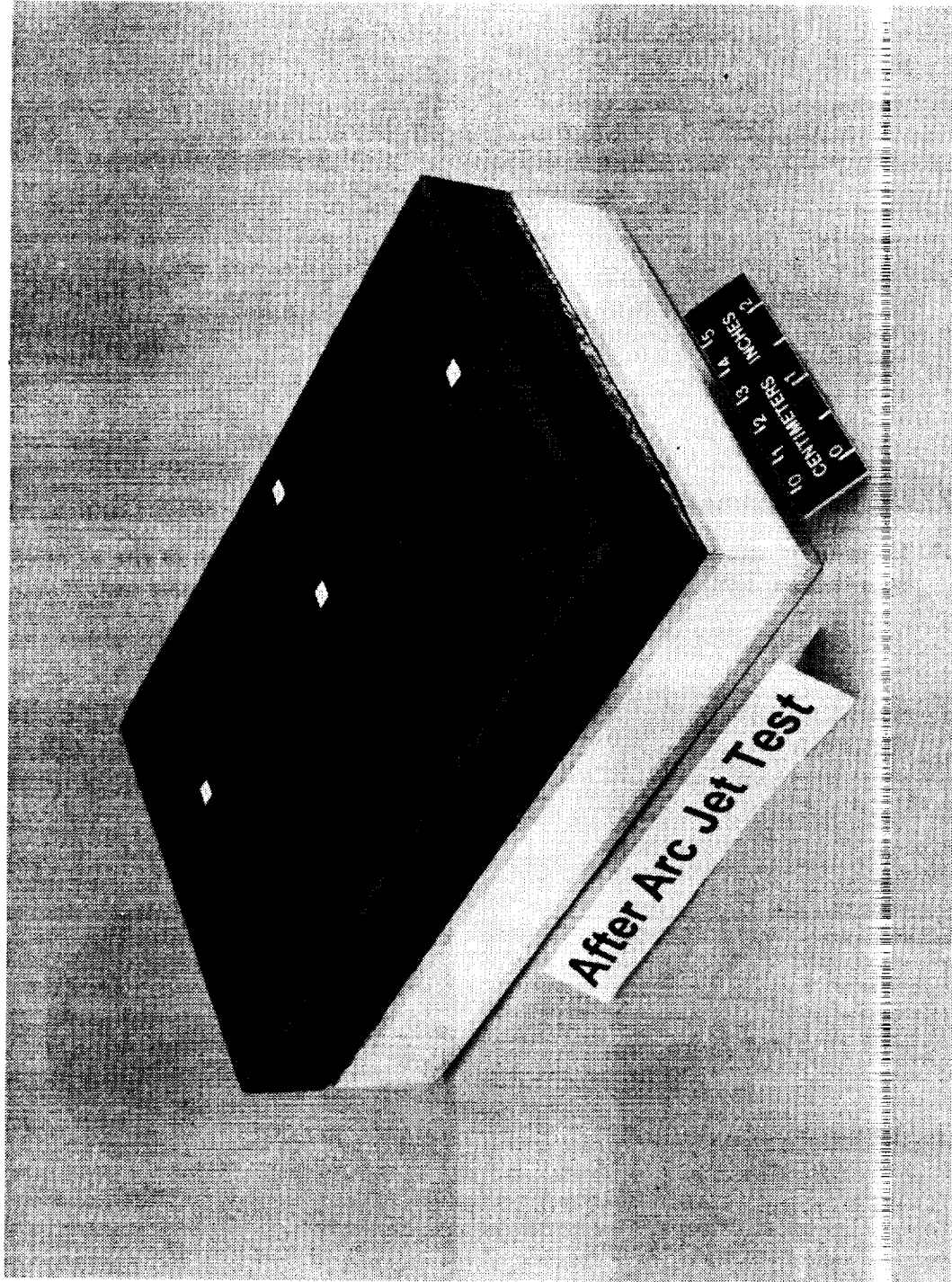


Figure 33. Isometric view of post-test tile.

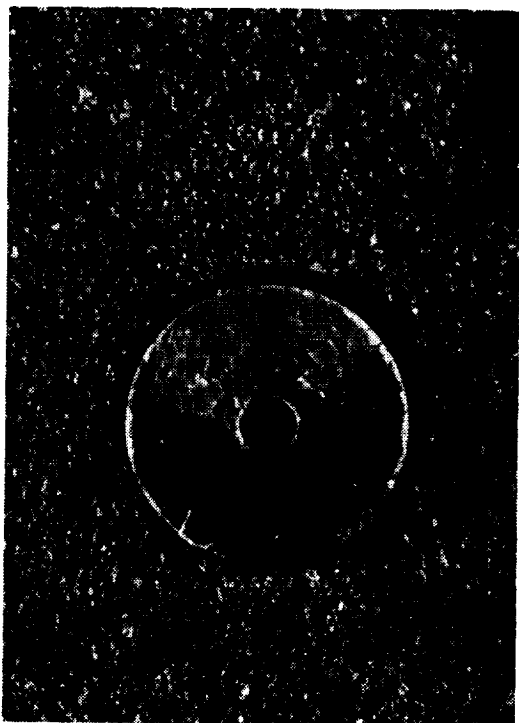


Figure 34. Close-up of site #1 after aero-thermal test.



Figure 35. Close-up of site #2 after aero-thermal test.



Figure 36. Close-up of site #3 after aero-thermal test.

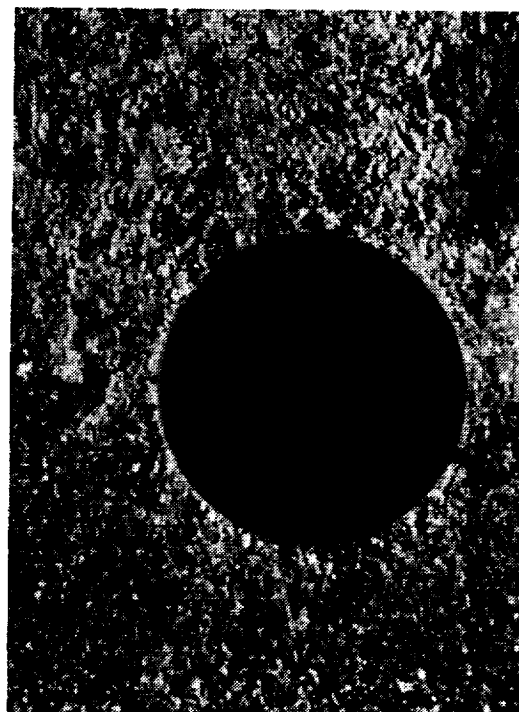


Figure 37. Close-up of site #4 after aero-thermal test.

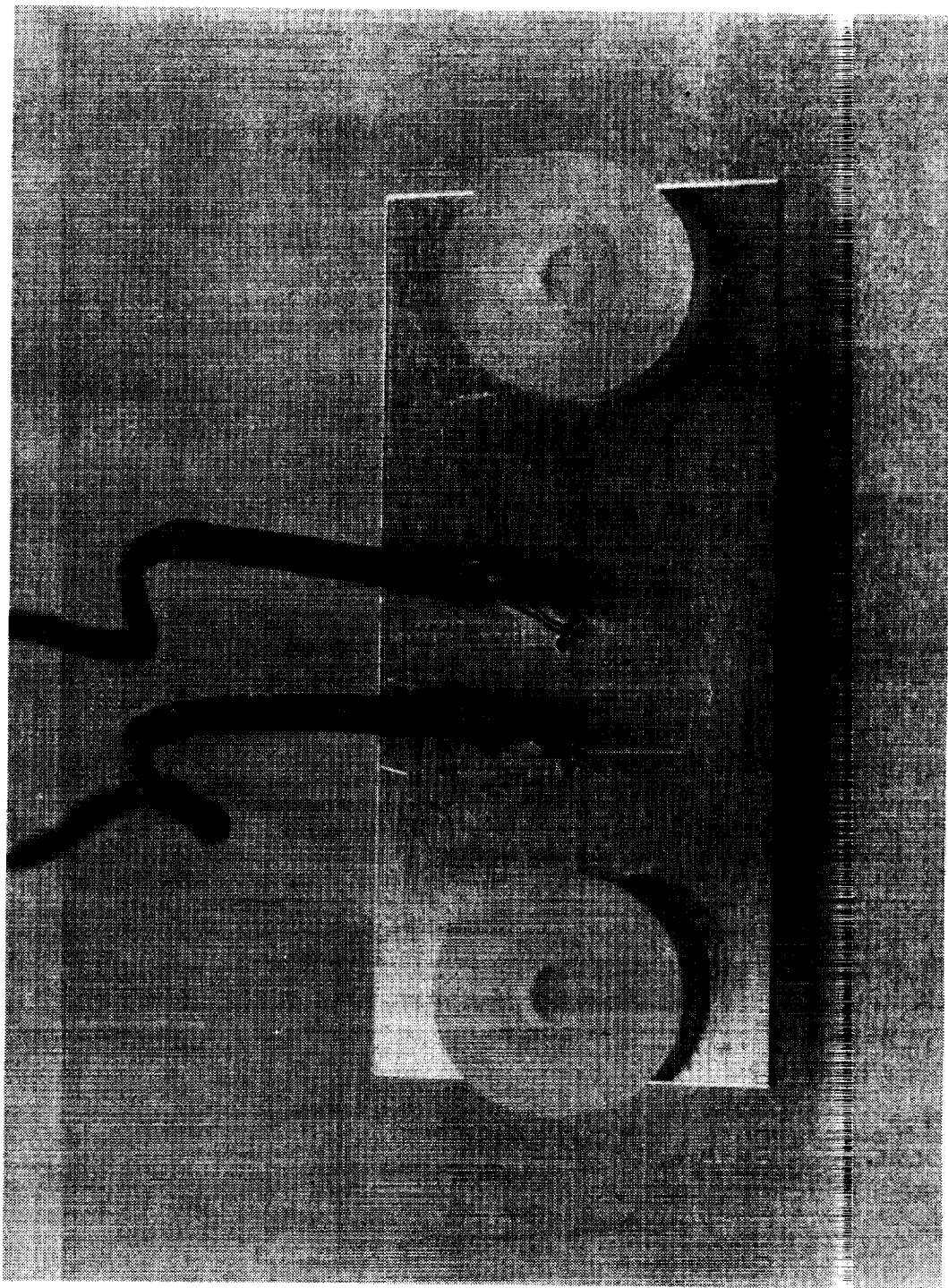


Figure 38. Calorimeter plate.



Figure 39. Cross section of the tile through site #2.



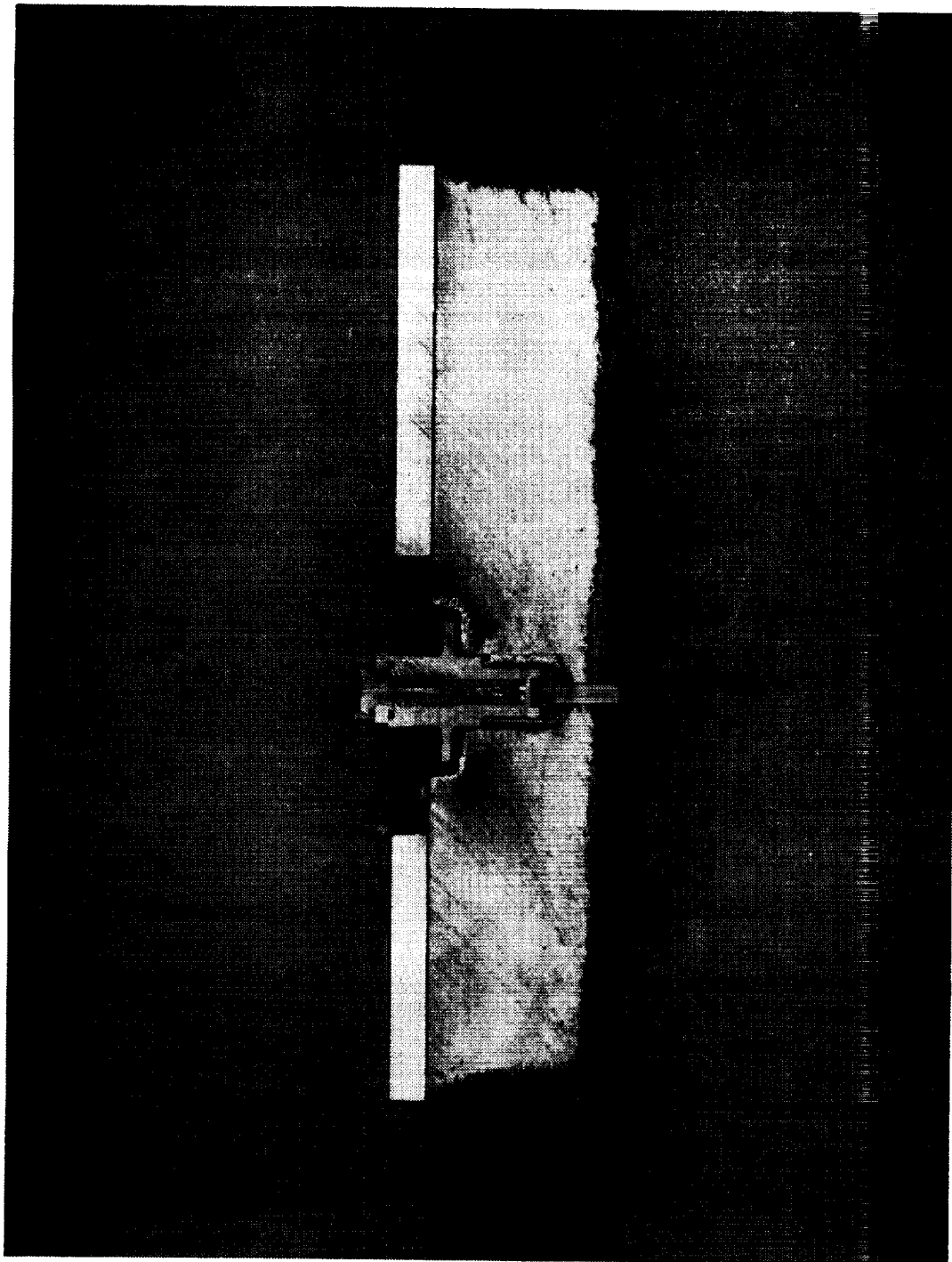


Figure 40. Cross section of the tile through site #3.

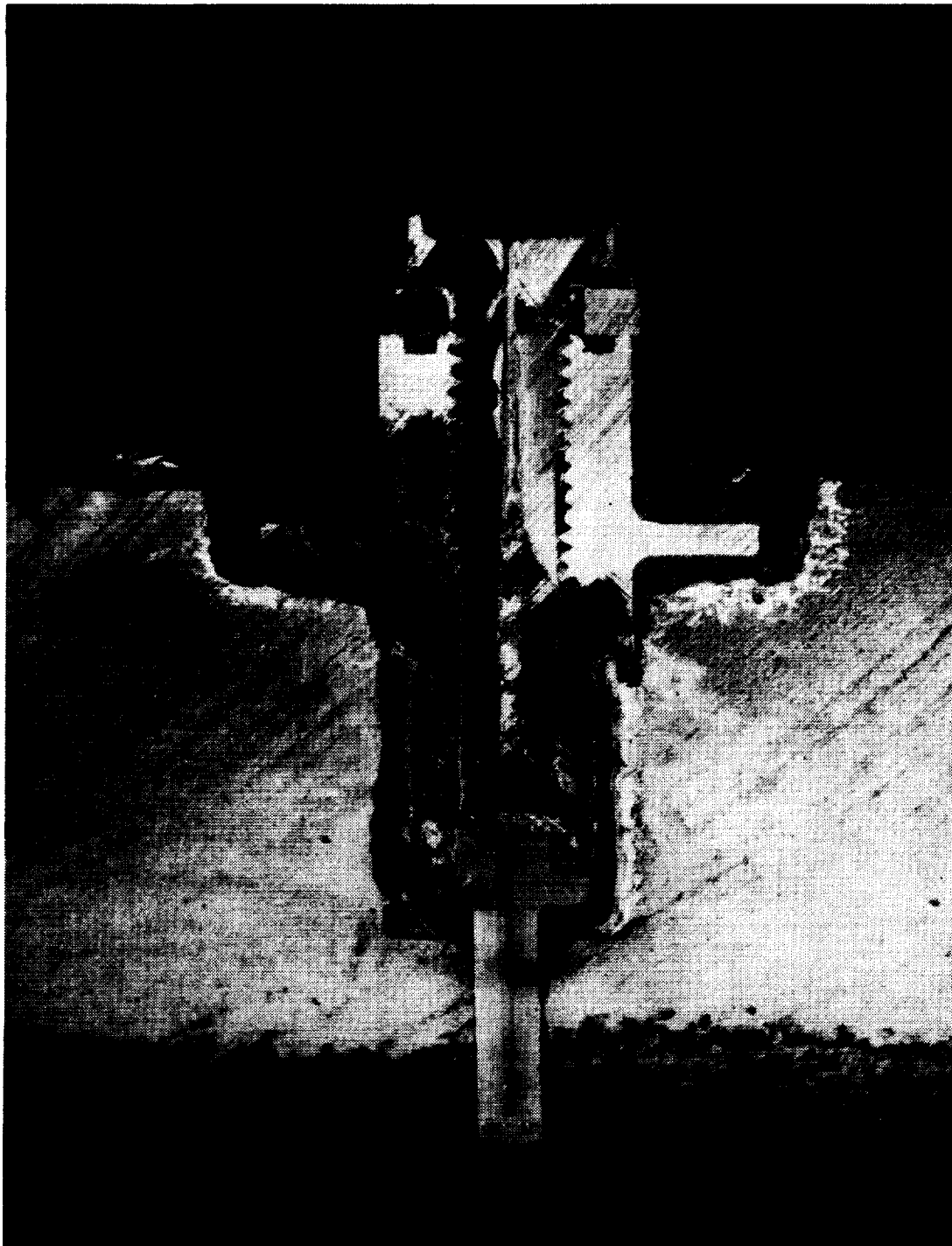


Figure 41. Close-up cross section of site #3.

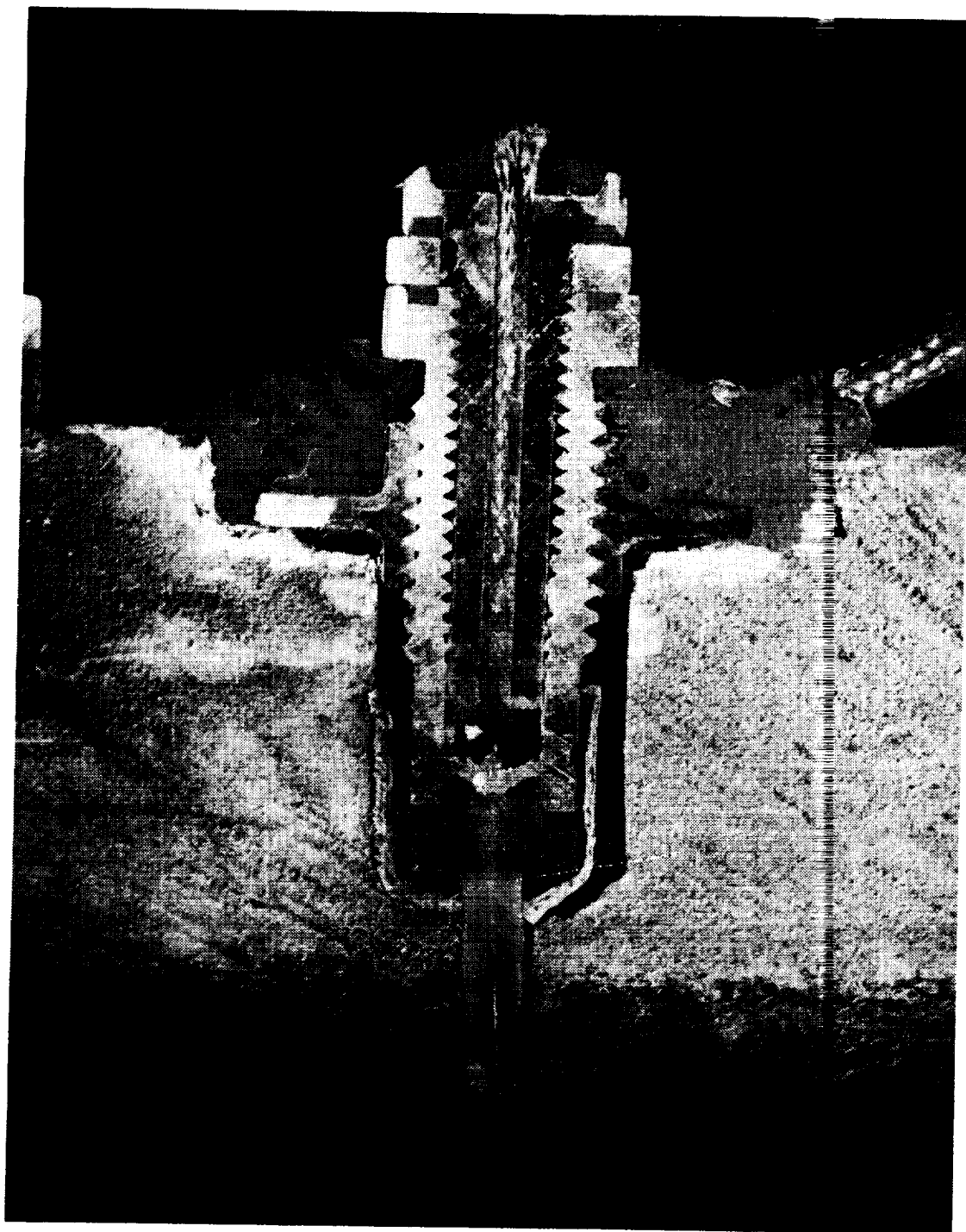


Figure 42. Close-up cross section of site #2.



Figure 43. Close-up cross section of thermocouple 9.

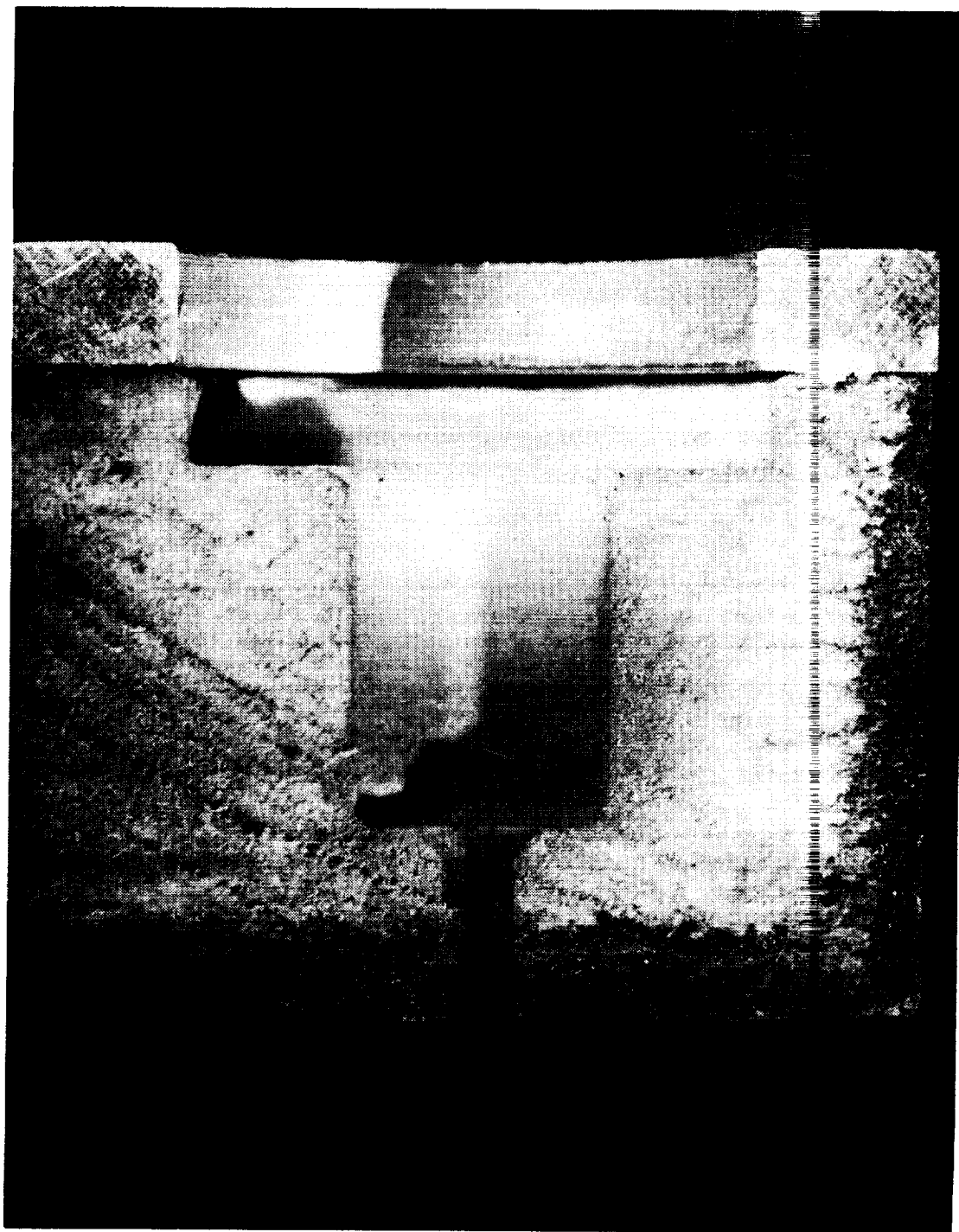


Figure 44. Close-up cross section of site #4.

# REPORT DOCUMENTATION PAGE

Form Approved  
OMB No. 0704-0188

Public reporting burden for this collection of information is estimated to average 1 hour per response, including the time for reviewing instructions, searching existing data sources, gathering and maintaining the data needed, and completing and reviewing the collection of information. Send comments regarding this burden estimate or any other aspect of this collection of information, including suggestions for reducing this burden, to Washington Headquarters Services, Directorate for Information Operations and Reports, 1215 Jefferson Davis Highway, Suite 1204, Arlington, VA 22202-4302, and to the Office of Management and Budget, Paperwork Reduction Project (0704-0188), Washington, DC 20503.

1. AGENCY USE ONLY (Leave blank)		2. REPORT DATE July 1994		3. REPORT TYPE AND DATES COVERED Technical Memorandum	
4. TITLE AND SUBTITLE Design and Evaluation of Candidate Pressure Ports for the HYFLITE Experiment				5. FUNDING NUMBERS 763-01-51-25	
6. AUTHOR(S) John E. Teter, Jr. Craig S. Cleckner Alfred E. Von Theumer					
7. PERFORMING ORGANIZATION NAME(S) AND ADDRESS(ES) NASA Langley Research Center Hampton, VA 23681-0001				8. PERFORMING ORGANIZATION REPORT NUMBER	
9. SPONSORING/MONITORING AGENCY NAME(S) AND ADDRESS(ES) National Aeronautics and Space Administration Washington, DC 20546-0001				10. SPONSORING/MONITORING AGENCY REPORT NUMBER  NASA TM-109146	
11. SUPPLEMENTARY NOTES Teter; Cleckner: Langley Research Center, Hampton, VA Von Theumer: Lockheed Engineering and Sciences Co., Hampton					
12a. DISTRIBUTION/AVAILABILITY STATEMENT Unclassified-Unlimited  Subject Category 19				12b. DISTRIBUTION CODE	
13. ABSTRACT (Maximum 200 words) A concept for placing a pressure transducer directly in a shuttle type tile was developed at Langley Research Center. A .5 inch long quartz tube with a .020 inch inner diameter provides the thermal isolation necessary to allow 2800°F surface pressure measurements to be taken by pressure transducer rated at 250° F. The assembly is potted in place with RTV 560 in a piece of FRCI-12 Thermal Protection System insulation tile. The integrity of the Thermal Protection System is maintained even with the intrusion of the pressure port assembly and the pressure port does not disrupt the air flow across the lifting body. Approximately 200 of these pressure ports are to be used in each of the HYpersonic FLight Experiment (HYFLITE) flight tests. Initial vibro-acoustic and aero-thermal testing of the pressure port designs have been completed at Langley Research vibration laboratory and the 20 MWatt 2 x 9 turbulent duct facility at Ames Research Center. The performance of the pressure ports were found to be well within the required design limits for all cases. In addition, a failure mode in which the entire pressure port assembly was removed proved to be a benign case.					
14. SUBJECT TERMS HYFLITE, pressure port				15. NUMBER OF PAGES 68	
				16. PRICE CODE A04	
17. SECURITY CLASSIFICATION OF REPORT Unclassified	18. SECURITY CLASSIFICATION OF THIS PAGE Unclassified	19. SECURITY CLASSIFICATION OF ABSTRACT	20. LIMITATION OF ABSTRACT		